Earth-Science Reviews, 24 (1987) 237–277
Elsevier Science Publishers B.V., Amsterdam—Printed in The Netherlands

Out of Our Depth: on the Impossibility of Fathoming Eustasy from the Stratigraphic Record

RANDE BURTON, CHRISTOPHER G.St.C. KENDALL and IAN LERCHE

ABSTRACT

Burton, R., Kendall, Ch.G.St.C. and Lerche, I., 1987. Out of our depth: on the impossibility of fathoming eustasy from the stratigraphic record. Earth-Sci. Rev., 24: 237–277.

The evolution of a sedimentary basin's gross morphology depends upon (1) basement movement, (2) sediment accumulation and compaction, and (3) variations of eustasy with time. Thus if an accurate history of eustasy could be derived, it would aid in our understanding of basin stratigraphy and help in the prediction of sediment geometry from described areas.

Techniques which attempt to determine the magnitude of eustatic sea-level excursions include the measurement of (1) the amount of sedimentary onlap onto the continental margins with and without the use of hypsometric curves, (2) the thickness of marine sedimentary cycles and the elevation and distance between indicators of old strandlines, (3) the perturbations on individual thermo-tectonic subsidence curves and stacked crustal subsidence curves, (4) the variations in deep-ocean oxygen isotopes found in sediments, and (5) the size of variables used in graphical and numerical simulations of basin fill in terms of tectonic behavior, rates of sediment accumulation and eustasy which "invert" the problem. To date a combination of the use of relative sea-level charts derived from sediment onlap of the continental margin with dimensioning by oxygen isotopes responding to glacial events offers the best potential for relative (tectono/eustatic) sea-level curves, but even this method can not produce a unique solution for absolute eustatic variations.

Mathematical modelling shows that, at best, it is possible to obtain only the *sum* of tectonic basement subsidence and sea-level variations from the above methods, and, at worst, not even that simple a combination. Thus, every proposed scheme to measure eustatic sea-level excursions *assumes* some behavior for two of the three underlying processes: tectonic movement of the basement, sedimentary accumulation and eustatic sea level. Each scheme then determines the third process relative to the assumed model behavior of the other two.

It would seem that, like King Canute, we cannot command the sea though we can still use undifferentiated "relative" (tectono/eustatic) sea-level curves to generate a "family" of solutions which are the product of a variety of absolute sea-level curves and tectonic models. Each solution has then to be assessed in terms of geologic setting and the hypotheses it generates.

INTRODUCTION

The importance of eustasy to basin history

The reader should note that the definition we use in this paper for eustasy is "a change in elevation in sea level on a worldwide basis relative to the stationary datum at the center of the earth". This definition may differ from those of other geologists cited in this paper.

Eustatic sea-level events are important to an understanding of basin history because they produce unique responses in the sedimentary record that can be recognized on a worldwide basis. They can date not only the sedimentary fill of specific basins but the fill from basin to basin. They modify depositional environments through time, and so are in part responsible from changes in the sedimentary record and the fauna which punctuate evolution (Hallam, 1984). Eustatic events can be used to identify relative sea-level changes, be they caused by (1) local tectonic events or (2) variations in the earth's rota-

0012-8252/87/$14.35

tional axis (Mörner, 1983). Should the rate of change of eustasy be more rapid than thermo-tectonic movements, then the size of the resulting accommodation for sediment fill can be ascribed to that sea-level change and may be used to predict the location and geometry of the sedimentary fill of basins. Finally, if the size of an eustatic event were known then this could help to determine how much of the crust's movement is related to flexural response to sea-level change versus thermo-tectonic subsidence.

Rande Burton graduated from M.I.T. with a B.Sc. in physics in 1965 and a Ph.D. in space science from U.C.L.A. in 1972. Worked as a geophysicist at Gulf Research in Pittsburgh from 1976 to 1982 on seismic stratigraphy, wave fauna analysis, work station technology and basin analysis including modeling eustasy. Currently (1982–present) at Standard Oil working on integrated interpretative work stations. Present address: Sohio Petroleum, Lincoln Centre, Suite 1200, Dallas, Texas 75240, U.S.A.

Christopher G.St.C. Kendall received his B.A. in 1962 and his M.A. in 1965 at Trinity College, Dublin, and his Ph.D. in 1966 at Imperial College, London. His main interests are in sedimentology-stratigraphy, and basin modelling, including sea level control on sediment deposition and the controls on carbonate deposition. He has spent a career working for both the oil industry and academia with work locations ranging from the United States, Great Britain, the United Arab Emirates, North Africa, and Australia. Most efforts have been devoted to Holocene and Ancient carbonates. Recent interests include Expert Systems and their role in hydrocarbon exploration. Present address: Department of Geology, University of South Carolina, Columbia, S.C. 29208, U.S.A.

Ian Lerche graduated from the University of Manchester, England, with a first-class honors B.Sc. in 1962, and with a Ph.D. in astronomy from the same institution in 1965. During 1965–1981, he was a member of the Physics Department faculty of the University of Chicago. In 1981 he was an employee of Gulf Research and Development Co. (GRDC), as a research associate in geophysics. Currently he is a geology professor at the University of South Carolina (Columbia, S.C. 29208, U.S.A.)

He received the Alfred P. Sloan Foundation Fellowship (1966–1968), and the Alexander von Humboldt Senior U.S. Scientist Award (1974–75). He was a visiting professor at M.I.T. (1975), visiting principal research officer at the Division of Radiophysics at C.S.I.R.O., Sydney, Australia (1977–1979), and visiting research scholar (GRDC) (1980–1981). He is a Fellow of the Royal Astronomical Society.

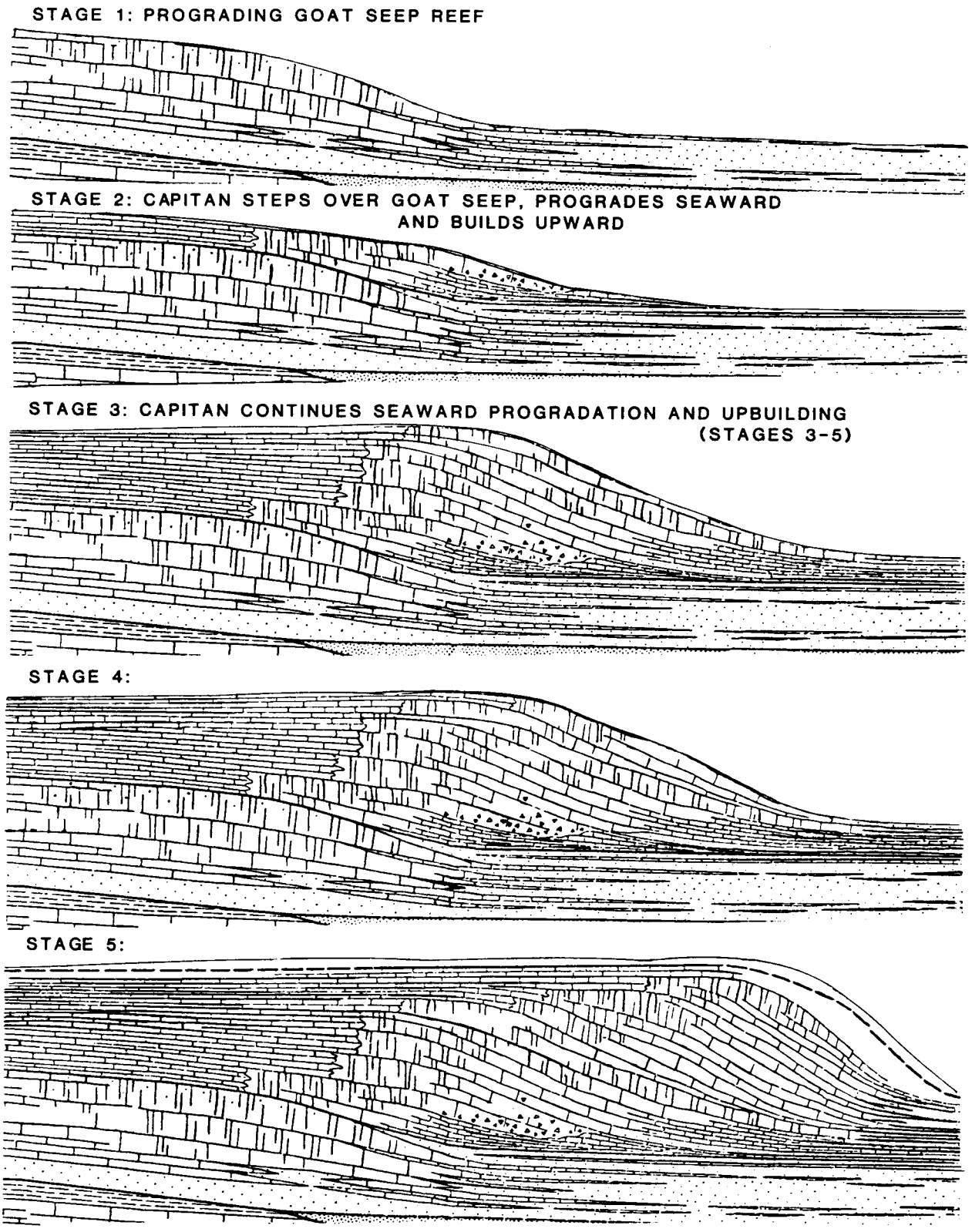

Fig. 1. Sediment geometry displayed by the Permian Upper Guadalupian margin of the Delaware Basin in west Texas and its evolution through time (after King 1948).

If, as we show in this paper, the record of absolute sea-level change cannot be untangled from sediment compaction, crustal flexural strength and thermo-tectonic behavior, then basin history modelling in the form of graphical simulations of the sedimentary fill can be used to yield a family of solutions. Geologic judgement is then applied to choose the most likely models and set limits on the input variables.

Later in the paper we provide the results of one such a simulation of sediment fill on a hypothetical continental margin. Similar simulations producing families of solutions could be useful as stratigraphic tools which would enhance our understanding of the stratigraphy of basins. For instance, a simulation might be used to duplicate sediment geometry during periods of over-the-shelf-edge sediment bypass during a low-stand as in the Lower Cretaceous of the North Sea or the Tuscaloosa of the Gulf Coast of the U.S.A; it could maximize the integration of geological, geophysical, and paleontologic data; and it could reinforce interpretations made from internal seismic reflections. The data required to do this can be derived from conventional sources such as biostratigraphic analysis, regional mapping, examination of core samples, well logs and seismic cross-sections. Such a simulation can be tied directly to oil and gas exploration. This strategy provides a dynamic framework of many possible solutions, from a variety of inputs, on which to superimpose depositional models to account for unconformities and lithological variation in vertical sequences, and to highlight the far-reaching effects of worldwide sea-level events. However, to construct such simulations we need to determine the magnitude of "relative" (tectono/eustatic) sea-level excursions to at least set limits to the possible solutions.

Major variables responsible for gross sediment geometry

The stratigraphy of the sediments that fill a basin is dependent on the source and depositional setting of the sediments, the role tectonism plays in controlling basin fill, and the influence of eustasy. It is the difficulty in separating these three influences that has plagued sedimentary stratigraphic interpretation and makes measuring the magnitude of eustatic sea level so difficult. Suess (1906), Stille (1924), Grabau (1936), Kuenen (1939), Umbgrove (1939), Bally (1981), Watts (1982), Matthews (1984a) and Hallam (1984) are among many geologists who have confronted the problem and have catalogued how, over the last 80 years, different people have tried to solve it.

As Goodwin and Anderson (1985) point out, the most pervasive component of stratigraphic sections is the "recurrent asymmetric sedimentary sequence". They cite the fining-upward "red bed" cyclothems of Allen (1964); the carbonate tidal flat cycles of James (1979); the clastic tidal flat cycles of Klein (1970); the deltaic cycles of Ferm (1970), and Walker and Harms (1971); and the submarine sequences of Ricci-Lucchi (1975). The problem is how one interprets these cycles. Some, like Horne and Ferm (1976) have argued that the cyclicity is largely a response to the lateral migration of depositional settings; others like Goodwin and Anderson (1985) favor eustasy, and still others like Fischer (1964) favor a tectonic cause.

The problem of resolving these different controls on sedimentary geology can best be demonstrated by trying to establish how a basin margin developed. For example, in Fig. 1 we have taken a slightly modified cross-sectional diagram by King (1948) in an attempt to see how the sediment geometries evolved in the carbonate and clastic sediments of the margin of the Upper Guadalupian Permian Delaware Basin in west Texas. At Stage 1, the margin began as a gentle ramp on which a massive fine-grained carbonate bank edge progressively built up and moved seaward over itself, while simultaneously interfingering seaward with basin clastics, and shelfward with shoaling-upward cycles of carbonates and clastics that are dominantly carbon-

ate close to the margin but become more clastic landward. At Stage 2, the margin suddenly stepped basinward with backreef carbonates lying abruptly over what was once the basin edge. The width of the belt where the massive basin margin sediments were deposited narrowed and the margin prograded gently seaward. The backreef maintained its general position while the margin prograded over a wedge of basin clastics. The same step-like jump seaward can be seen in Stages 3, 4 and 5.

The problem facing the stratigrapher is to explain the geometries and facies seen in this geological cartoon. Consider three different hypotheses that account for the observations.

Hypothesis 1. If we subscribe to the belief that depositional environments migrated along depositional strike, the cause of both the shoaling-upward cycles and the step-like progradation could be a response to lateral shifts in the site of active carbonate sedimentation on the shelf. At locations away from localized sites of active carbonate sedimentation, clastic bypass into the basin was achieved through dense lagoonal brines (Harms, 1974; Williamson, 1977). Subsequently, the return of the carbonate "factory" produced the shoaling upward cycles and local progradation.

Hypothesis 2. The tectonic subsidence which created the "accommodation" (space between a base level related to sea level and the sediment–water interface) for the sediment of the shelf margin did not change at a constant rate but instead accelerated and decelerated periodically. Slow acceleration of tectonic subsidence would initially have caused the shelf carbonates of Stage 1 to maintain their general slow progradation. A rapid deceleration in subsidence would have resulted in Stage 2 in a reduction of accommodation for the sediment. Rapid progradation would have occurred until another abrupt acceleration phase in subsidence.

Hypothesis 3. This hypothesis involves eustatic control. At Stage 1 the observed progradation took place during a moderate eustatic rise. The adjacent basinal clastics were then deposited during a rapid eustatic fall which also provided the conditions for aeolian transport of the sands over the shelf into the basin. The following rapid seaward stepping of the shelf carbonates of Stage 2 could have been the result of a rapid eustatic rise during which the coast retreated, while carbonate sediments onlapped the shelf and a condensed sequence formed offshore. This rapid event was followed by a very slow eustatic rise which produced little accommodation, so that seaward stepping of the shelf resulted; and so on with the other stages.

Supporting evidence can be found for each of the hypotheses we have used to explain the geometries observed in the Delaware Basin margin (Table I), but, as will be seen as the paper progresses, no conclusive proof seems to be available for any one of them.

Similar confusion results if one tries to explain clastic cycles from an epeiric sea setting. These cycles, too, have been interpreted as being produced by (1) switching of point sources or sediment (Horne and Ferm, 1976), (2) spasmodic subsidence, (3) alternate subsidence and uplift, (4) eustasy (Wanless and Shepard, 1936). Wells (1960) was even more imaginative and listed more interpretations but favors eustasy while admitting a lack of proof. Unfortunately, as with the carbonate cycles, none of the hypotheses can be supported.

Taking it further, based on the literature referenced in this paper and the mathematical formulation for the forward model of sediment basin fill presented later, in most cases the cause of the cycles we see in sedimentary sections remains unresolved and interpretation is very much a response to geologic fashion rather than to definitive data. An objective of our original study was to resolve the size of (1) eustatic excursions, (2) tectonic movement and (3) rates of sedimentary accumulation. Our contention is that if the size of two of these variables could be determined then there is a chance of establishing the size of the third. Only then could one determine

TABLE I

Evidence for and against the three hypotheses presented to explain the sedimentary geometries seen in cross-sections of the Delaware Basin margin, West Texas

Hypothesis	Evidence	Explanation
(1) Switching of location	*For*:	
	Shoaling up cycles	High carbonate production active at site of cycle.
	Clastics on shelf and in basin	Carbonate production turned off, clastics transported by wind and dense brines.
	Shales in basin	Both carbonates and clastics turned off, so shale no longer overwhelmed by other sediment, and its accumulation is more obvious.
	Against:	
	Apparent continuity of carbonate cycles down dip. Basin wide shelf sand with no contemporaneous carbonate production	Accommodation for carbonate and sand bodies produced by eustasy or tectonic movement; however, widespread cycles may be exception, so source switching may be dominant mode of sediment origin.
(2) Tectonic dictator	*For*:	
	Shoaling up cycles	Relative sea-level rise caused by spasmodic tectonic subsidence creates accommodation for cycle.
	Clastics on shelf and in basin	Relative sea-level still stand or drop caused by tectonic still stand or uplift exposes shelf above sea level and wind transports sand onto shelf and across it into the basin.
	Shales in basin	Rapid relative sea-level rise caused by rapid tectonic subsidence creates too much accommodation on shelf and basin starvation results.
	Clastic and marine fill of fissures	During exposure explained above, basin margin is not supported by buoyant water and so fractures. These cracks are filled by aeolian clastics and marine carbonates.
	Evidence of subaerial exposure 20 m below crest of bank margin in Yates shelf crest in Walnut Canyon (R. Sarg, pers. commun., 1986)	If tectonic uplift exposes margin of bank then subaerial weathering should be seen.
	Against:	
	No downslope shallow carbonates	If tectonic uplift exposes bank margin, shallow water setting should be shifted downslope.
	Cycles can be traced outside basin	Either tectonic events extend beyond basin or eustasy is responsible.
(3) Eustatic sea level	*For*:	
	Shoaling up cycles	Eustatic sea-level rise creates accommodation for cycle.
	Clastics on shelf and in basin	Eustatic still stand, or relative still stand in response to eustatic fall exceeding tectonic subsidence exposes shelf and wind transports sand on shelf and into the basin
	Shales in basin	Rapid relative rise caused by eustatic rise, coupled to tectonic subsidence, creates too much accommodation on shelf and basin starvation results with shale deposition only.

TABLE I (continued)

Hypothesis	Evidence	Explanation
	Clastics and marine sediments fill fissures	During exposure (explained above) basin margin is unsupported by buoyant water and so fractures. These fractures are filled by aeolian clastics and marine carbonates.
	Evidence of subaerial exposure 30 m below crest of bank margin of Yates shelf (R. Sarg, pers. commun., 1986)	Subaerial exposure should be seen with relative sea-level fall.
	Cycles traced outside basin	Eustatic sea-level rise effects would be seen beyond one basin.
	Against:	
	No evidence that these are the same cycles.	Suggests tectonism or spasmodic switching is responsible.
	No downslope shallow carbonates	If shallow shelf exposed then shallow setting shifted downslope.

Note. Though current geologic thought trends towards a eustatic sea-level control, no unequivocal case has yet been presented. Probably all three mechanisms worked at one time or another through the Upper Guadalupian but no proof of this has been identified in the field by the authors or has been recorded in the literature they have read.

how a basin filled and what caused sedimentary cyclicity.

As a result of these objectives we decided to investigate the different methods of determining the magnitude of eustatic excursions in the hope we could use one, or all of them, to provide the data we needed for a graphical simulation. The next sections show the results of this study.

SOME METHODS WHICH PURPORT TO MEASURE THE MAGNITUDE OF EUSTATIC EXCURSIONS

Though several indirect methods for determining the size of eustatic events exist, no direct method of measuring eustatic changes has ever been derived because of the lack of a stationary datum from which these changes can be measured. This datum cannot be established because the earth's surface has a history of constantly moving in response to (1) sediment compaction, (2) the isostatic response of the crust to varying load of the sedimentary and water columns that rest upon it, and (3) thermo-tectonic movement. Vella (1961) points out that apparent changes in the height of sea level can only be expressed as the height between pairs of four kinds of vertical reference points, none of which are fixed, and all of them subject to vertical movement. These are (1) any point at mean sea level, (2) any point fixed relative to the lithosphere, (3) any point on the changing surface of the lithosphere, and (4) any point on the near compaction surface slightly below any depositional surface. It is because no direct measurement can be made that geologists are forced to construct models which use measurements of the physical changes that sea-level movements produce. It is these indirect measurements, which are related to the magnitude of eustatic change, that are the subject of this paper.

Gutenberg (1941) faced this problem when he tried to determine the size of changes in sea level using tide gauge data collected over a number of years from all over the world. Due to variations in crustal motion he was forced to assume an "average" sea-level change compiled from all his observations. In areas of postglacial rebound he used this

"average" value to separate out the uplift of the land. However, his results were only relative since there was no fixed datum from which to measure his sea-level variations.

Suess (1906) was one of the first geologists to recognize the importance of movements of eustasy and their effect on the deposition of marine sediments. He described eustatic movements as being changes in the level of the strand, which were of equal height and which occurred on a worldwide basis. He recognized the difficulty of separating "relative" sea level (Chambers, 1848) from eustatic changes, and wrote a review on the subject which begins by citing Dante speaking in 1320 on the problems of sea level with respect to the curvature of the earth and the elevation of the land.

Suess (1906) described three means of recognizing changes in sea level which include (1) the different positions of the old strandline sediments deposited by ancient seas on the continent, (2) the paleo-bathymetry of sedimentary formations, and (3) the elevation of old strand lines with respect to the present coast. His review focused on explanations of changes in eustasy and the problems of measuring them. He described the repeated synchronous transgressions and regressions found in the sedimentary record from all over the world and expressed the opinion that these were independent of secular oscillations in the continental crust. Significantly, he postulated that the unconformities used by William Smith to demark formations were related to eustatic sea-level falls.

By 1916 Schuchert had used synchronous marine sediment packages that onlapped the continent to produce one of the first relative sea-level charts, which showed the percentage of the North American continent covered by the sea through the Phanerozic (Fig. 2). He ascribed these sea-level changes to continental diastrophism. Stille (1924) also felt that these synchronous changes in sea level could only be understood in terms of synchronous movements of the continent, and in conjunction with Lotze from Berlin also constructed sea-level charts. However, the size of the sea-level excursions identified by Stille (1924) and later by Umbgrove (1939) remained a problem. Their relatively size could be recognized by determining how much of the continent was onlapped by the sea but the height of the sea-level movement was still unknown. Kuenen (1939) alludes to a system of estimating the size of these sea-level excursions in terms of a hypsometric curve (in other words the percentage of continent that would be above sea level for each unit rise in sea level). The system requires tracing the edge of a dated onlapping marine sedimentary wedge and then presupposing a relationship between the relief of the continent and its area, and using this to determine how high sea level stood at this time. Since these early works, probably the most commonly used means for estimating sea-level variations has been based on this hypsometric system.

Recently Vail et al. (1977) using seismic

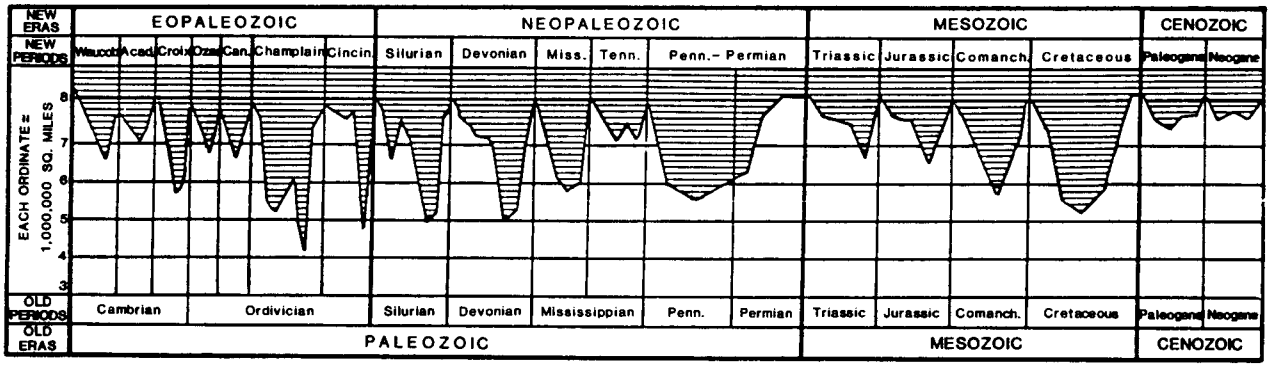

Fig. 2. Marine encroachment chart for the Phanerozoic of North America (after Schuchert, 1916).

stratigraphy have developed a method for estimating heights of sea-level variation, which appears to have replaced the hypsometric curve in popularity. Another system, similar to Vail et al.'s, is related to the measurement of the thickness of depositional cycles and their geometry across the continent. A further method relates the crustal response to the weight of sea water (Van Hinte, 1978; Watts and Steckler, 1979; Guidish et al., 1984).

The final system for estimating heights of sea-level variation is related to attempts to measure changes in the volume of sea water. These measurements are largely related to glacio-eustatic changes in sea level produced by fresh water being frozen and forming ice floes over the higher-latitude oceans and large continental ice caps covering the higher-latitude continental areas. The freezing of large volumes of fresh water lowers sea level and produces changes in the chemistry of sea water that may be reflected in the trace element and isotopic composition of the minerals associated with the marine sedimentary record. Oxygen isotopes in benthic foraminifera are the major indicator used in this system. The isotopic ratio (δO^{18}) increases in a predictable manner in the ocean when an ice cap forms (Shackleton and Opdyke, 1973; Matthews, 1984b). This is because the ocean becomes a sink for the heavier oxygen isotopes while the light ones are preferentially transported by evaporation and precipitation to the ice cap. As a result oxygen isotopic ratios (δO^{18}) are used to try to determine the magnitude of the sea-level change.

The volume of the ocean may also be determined from its relationship to the decreasing speed of the rotation of the earth which can be estimated beginning from the time the Babylonians began keeping records around 500 B.C. (Morrison, 1985). The day is now 50 ms longer. The torque caused by tides has not changed appreciably since then, so some other mechanism is responsible. "For example a change in sea level of 1 m would alter the length of the day by 15 ms" (Morrison, 1985). So possibly the sea level has risen by 3 metres since 500 B.C. This change in sea level is supported by archeological and geological evidence from the coast of Georgia (De Pratter and Howard, 1981). However, other mechanisms ranging from tectonics to deep crustal changes may be responsible too.

Our paper considers five methods which are used to describe the earth's physical response to eustasy: (1) the changing area of the continents onlapped by the sea; (2) the marine sediment depositional record; (3) the crustal response to the weight of the onlapping sea water; (4) the changing volume of ocean water; and (5) a forward modelling approach which considers tectonic movement, rate of sediment accumulation and eustasy. We now review these five methods.

Use of the changing area of continents covered by marine sediments to determine the amplitude of eustatic excursion

(A) *Hypsometric curves.* Kossinna (1921, 1933) compiled hypsometric curves for the present-day topography of the continents. His curves, and others based on his modified concepts, have been the basis for many estimates of the magnitude of excursions in eustasy. The present-day hypsometric curve is one means by which one can estimate how much the sea level rose in proportion to the area of the continent covered by the sea. Using a planimeter and an equal area projection the amount the sea advanced across the continent during any particular time interval can be derived from paleogeographic maps of the marine sedimentary sequences for that time period. A number of recent papers by Eyged (1956), Hallam (1963, 1984), Forney (1975), Bond (1976, 1978a, b), Cogley (1981, 1984), Harrison et al. (1981) and Wyatt (1984) all describe the use of the hypsometric curve (or the hypsographic curve) in the determination of the size of sea-level excursions.

The hypsometric curve expresses the area of land between pairs of contour lines as a percentage of the total land area. For instance, Harrison et al. (1981) made their plots

using the fractional area versus fractional height and included the continental shelf area. They normalized the curves by dividing the observed height by the observed average height which is expressed as an ordinate on their plot so that the average height is therefore unity and the area is a percentage of the total area of the continent (Fig. 3).

The problem with this method of determining the magnitude of sea-level rise or fall is that it presupposes that the hypsometric curve that describes a continent today is the same as that which existed in the past. However, the way this simple concept is applied varies from scientist to scientist. Present-day curves (e.g., Kossinna, 1921, 1933) may be oversteep

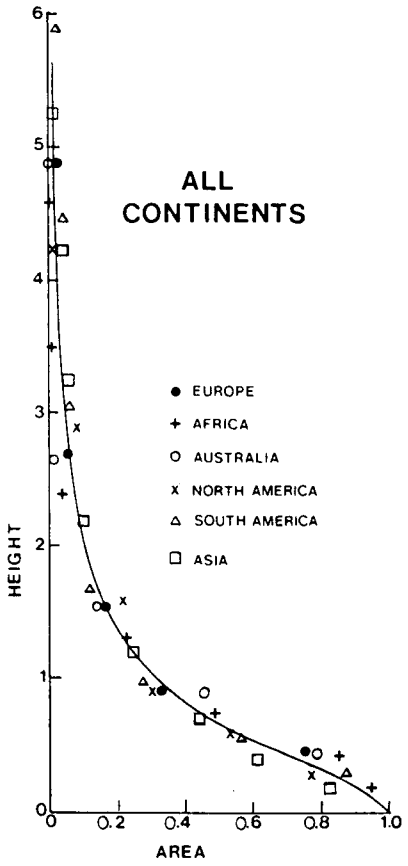

Fig. 3. Normalized hypsometric curve after Harrison et al. (1981). "The continental heights are normalized by dividing observed height by average height. The average height of each continent would therefore be plotted as unity on the ordinate scale. Area is unity on the abscissa scale. The best fitting hypsographic curve through these points is also shown".

due to epeirogenic uplift in the Tertiary (Bond, 1976). According to Harrison et al. (1981) the hypsometry of a continent is unlikely to be constant through time because of (1) changes related to the sediment fill of the continent margins, (2) the effects of fold mountain generation, and (3) problems in constructing hypsometric curves such as not including the continental shelves in the continental area covered by the hypsometric curve.

Cogley (1981) considered that the paleogeographic maps used in conjunction with the hypsometric curve are often in error, particularly when an older geologic system is mapped. He felt there is a bias towards drawing shorter simpler shorelines with the consequent underestimation of the areas of continent flooded back in time. He also pointed out that if the time interval used for making the paleogeographic maps varies then the paleogeographic maps for longer time intervals can show a greater onlap than those for shorter time intervals. As with Harrison et al. (1981), Cogley (1981) also recognized that orogenic thickening will change the relief expressed by the continent. He suggested parts of continental shelf areas may have been exposed in the past, but due to lack of stratigraphic information a wider transgression is assumed when in fact, it may have been more limited. He pointed out that the models of the continental reassemblage used by different scientists vary and produce different continental areas and different hypsometric curves. In much the same vein Wyatt (1984) noted that continents with larger areas will stand higher above sea level than those with smaller areas because they have larger volumes. Thus Pangea with its greater area, and so volume, stood higher than would be predicted from the present-day hypsometric curve.

To conclude, "modern area–altitude distribution provides important clues to that of ancient continent" (Cogley, 1984) and can be used as a system of modelling to determine the magnitude of sea-level excursions. However, there is no unequivocal way of deriving the "correct" hypsometric curve. One can use

those of Kossinna (1921, 1933), Bond (1976), Southham and Whitman (1981), Harrison et al. (1981), or Cogley (1984), or one's own system. Thus it is clear that the inaccuracies of paleogeographic mapping alone will result in inexact sea-level relationships, though some useful relative curves may result. Thus, like Hallam (1981), one could use the hypsometric curve to derive a sense of the gross relationship of sea level to continental area. Alternatively one can map areal curves, as Hallam (1963, 1969 and 1977) did for the Jurassic, which like those of Schuchert (1916), at least show relative sea-level positions. Bond (1976, 1978a,b) has used "average" curves effectively to track continental subsidence in North America in the Late Cretaceous and to show that Africa was probably uplifted through the Tertiary. Similarly Pitman (1978) and Kominz (1984) referred in part to hypsometric curves as well as onlap curves compiled by Rona (1973) when predicting the magnitude of eustatic changes and modelling the size of oceanic ridges during sea-floor spreading. As it is, then, the hypsometric curve can be considered for use as a general baseline from which to measure an overall sea-level rise through the Phanerozoic, and a means for looking at relative magnitudes of sea level.

(B) *Sediment aggradation and onlapping geometries from seismic stratigraphy.* Vail et al. (1977, 1984) and Hardenbol et al. (1981) have developed two of the best known systems for attempting to determine the size of sea-level changes. These are (a) the determination of the position of onlapping sedimentary wedges of marine, coastal and alluvial sediments on the continental margin through geologic time from seismic cross-sections, and (b) the measurement of the size of perturbations on crustal subsidence curves when compared to thermo-tectonic models. We consider the first system in this section and the second system in a later section.

Vail et al.'s (1977) technique is an extension of the work of Wheeler (1958), Sloss (1963, 1972) and Sloss and Speed (1974) and is used to identify seismic sequences on seismic cross-sections assuming that continuous seismic reflectors on acoustic geophysical cross-sections are close matches to chronostratigraphic surfaces, or time boundaries such as bedding planes and unconformities. The unconformities that bound the sequences are demarked by seismic reflectors onlapping and terminating either against the lower unconformity surface or against each other (Fig. 4). The argument here is that the position of the onlapping seismic reflectors is controlled by the base level of the mean high water mark. Thus a sediment (or seismic) encroachment chart can be drawn that shows how far the sediment wedge of submarine, coastal and alluvial sediment has onlapped the basin margin (Vail et al., 1977). A sediment (or seismic) aggradation chart can also be constructed that shows the vertical component by which onlapped seismic reflectors have climbed or fallen (Fig. 4c) (Vail et al., 1977). Vail et al. pointed out that in using this method "the measurements of coastal aggradation are made as closely as possible to the underlying unconformity to minimize the effect of differential basinal subsidence". They then correlate the cycles of relative changes of sea level at multiple locations and construct charts that incorporate the occurrence of global sediment (or seismic) onlap cycles. Using the aggradational measurements from the seismic, Vail et al. estimated the magnitude of relative sea-level excursions. However, as Hardenbol et al. (1981) pointed out, "quantifying eustatic sea-level changes from measured changes in coastal onlap does not provide an accurate measure, because of variations in subsidence in different basins". However, they presumably assume that once subsidence is factored out through geohistory analysis, in theory only eustasy remains. It should be remembered, though, that this is a hope rather than fact. As we show later in the paper, when we discuss the simulation, not only do crustal subsidence and compaction vary from basin to basin but their effects can cause as much as five times exaggeration to the sediment onlap curves.

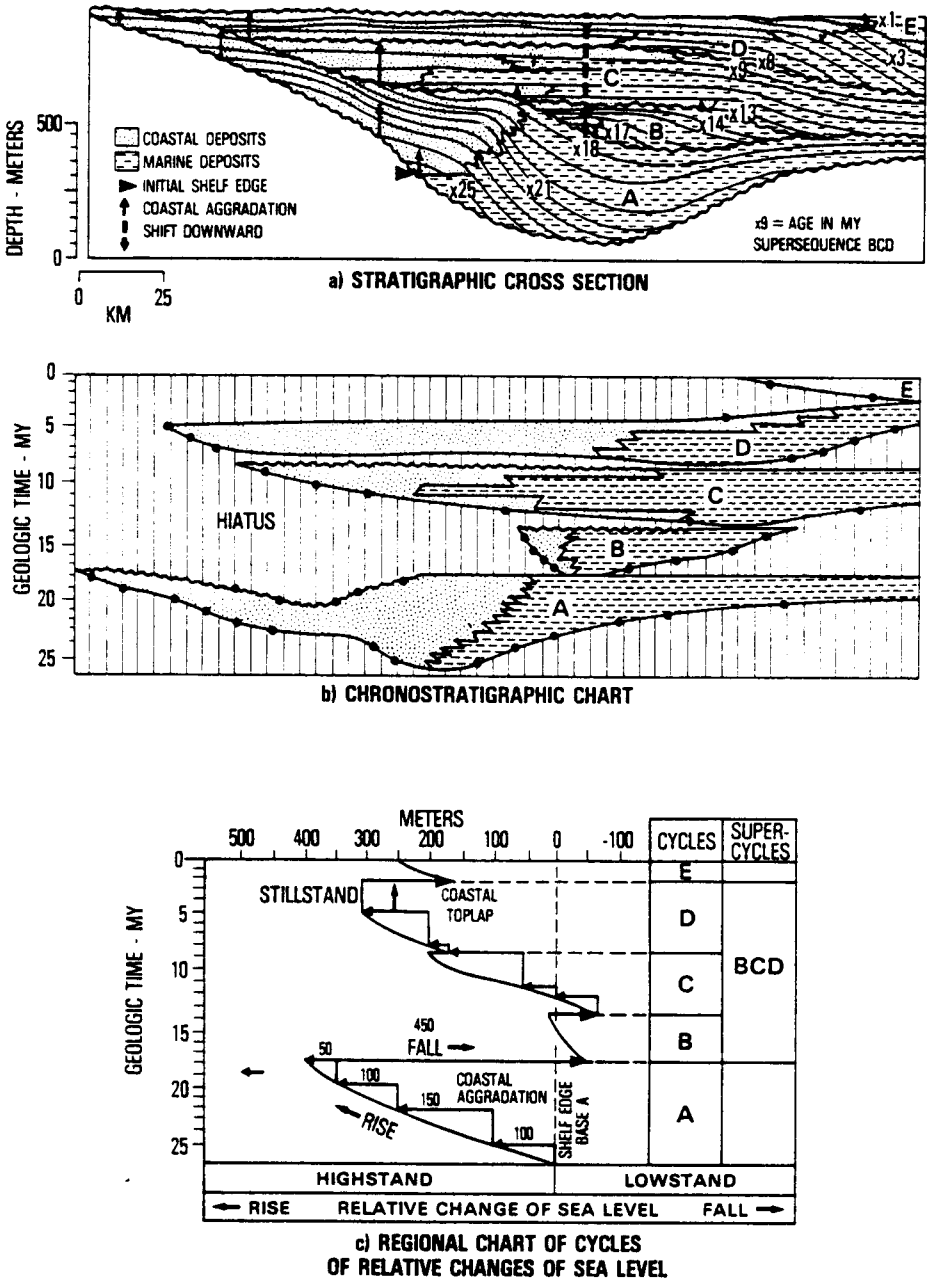

Fig. 4. a) Diagrammatic stratigraphic cross-section across a hypothetical seismic cross-section, showing distribution of sequence boundary types, downlap surfaces (condensed sections) and general facies of idealized sequences in depth. b) Chronostratigraphic chart or Wheeler diagram (Sloss, 1984; Wheeler, 1958) identified in a), showing nature of sequence boundaries, downlap surfaces and condensed sections, and facies.
c) Chart of cycles of relative changes of sea level constructed from a). Note arrows of coastal aggradation transferred to c). a), b) and c) after Vail et al., 1984.

A further problem with the sediment (or seismic) onlap curves of Vail et al. (1977) is that while they could be a product of eustasy they may alternatively be a product of regional tectonic movement or both (Bally, 1981; Watts, 1982; Thorne and Watts, 1984; Parkinson and Summerhayes, 1985; Miall, 1986). While we believe that Vail et al. (1977) have convincingly demonstrated the existence of their eustatic events, we think that the

position an eustatic event had on the continent is complicated by the local effects of tectonic subsidence (Bally, 1981; Watts, 1982; Thorne and Watts, 1984). This may explain why sea-level curves for the Jurassic compiled by Hallam (1981) and Vail and Todd (1981) from different data sources record different positions for the same sea-level stands. Similarly sea-level curves for the Cretaceous compiled by Vail et al. (1977), Kauffman (1977), Hancock and Kauffman (1979), Harris et al. (1984), and Seiglie and Baker (1984) from different data sources, (e.g., seismic, lithostratigraphic and biostratigraphic data) are also different. Also sea-level curves for the Late Tertiary compiled by Vail et al. (1977) differ from those of Seiglie and Moussa (1984). Thus these methods (which are used differently by the separate authors) recognize the occurrence of the same eustatic events but cannot be used to determine their magnitude, or their position with respect to other sea-level events. One could argue that the Vail et al. (1977) curves are global while those of the other cited authors are regional, so of course they differ. The problem is that Vail et al. (1977) have had to assume an "average" crustal subsidence to remove the "local" tectonic noise.

Matthews (1984b) has come up with an elegant possible solution in which he suggests using the oxygen isotope record from the last 100 Ma to dimension the relative size of the events identified by Vail et al. (1977), Vail and Hardenbol (1979) and Vail et al. (1984). This presupposes (1) that there have been glacial events as far back as 100 Ma, and (2) that the oxygen isotopes of skeletal remains of benthic fauna solely represent these events.

Some geologists question whether seismic reflectors are close approximations to bedding plane surfaces and so to chronostratigraphic surfaces or isochrons. Like Hallam (1984), we believe that bedding planes and so seismic reflectors must transgress time but, *in contrast* like Vail et al. (1977), we believe both parameters can also be used to subdivide strata into relative time packages, with the sediment lying beneath a bedding plane or seismic reflector being generally older than the sediment above. This concept has been tested and is used by hundreds of oil company geologists and geophysicists every day tying synthetic seismic traces constructed from sonic logs (Sengbush et al., 1961; Gardner et al., 1974) to seismic cross-sections. They identify chronostratigraphic horizons on the sonic logs and tie these to reflectors on the seismic cross-sections, tracing the stratigraphy from well to well (Vail et al., 1977). Gairud et al. (1978) used this system to determine the Tertiary stratigraphy across the Jan Mayen Ridge in the Norwegian–Greenland sea using multichannel seismic and DSDP wells. In the same way Schlee and Fritsch (1983) and Poag and Schlee (1984) were able to use seismic lines and COST wells to begin unravelling the seismic stratigraphy of the Georges Bank Basin and the Atlantic margin. Though they were unable to recognize all the unconformities and hiatus on the seismic lines that they identified in the wells, they were able to trace some. Von Rad and Exon (1983), using seismic and well data, dated seismic sequences and were able to work out the paleoenvironmental and geodynamic evolution of offshore northwest Australia. Similarly Willumsen and Cote (1983), using many wells tied to regional seismic lines, were able to work out the Tertiary sedimentary history of the southern Beaufort Sea. Other papers by Harding and Lowell (1983), Hamberg (1983), Cook et al. (1983), Curnelle and Marco (1983), Phelps and Roripaugh (1983), Kirschner et al. (1983), Suzuki (1983), Dimian et al. (1983), Erxleben and Carnahan (1983), Thomson (1983), Stone (1983a,b), Pieri (1983), Bachmann and Koch (1983), Norton (1983), Fox (1983), Harding et al. (1983), Rafavich et al. (1984), Gamboa et al. (1985), Harding (1985), and Crain et al. (1985), have also recorded the method and report how wells are tied to seismic reflectors to interpret the seismic stratigraphy and structure of the subsurface. Van Hinte (1983) not only accepted in general that seismic reflectors can be equated to isochrons, but went

even further and used well data to produce "synthetic" seismic sections by projecting biostratigraphically controlled markers or isochrons from well to well, as if they were seismic reflectors. Other workers, like Middleton (1984), use seismic reflectors as "isochrons" to model "pseudo" wells at common depth point, wiggle trace locations (CDP's). The "dated" reflectors provide the pseudo-well stratigraphy so that "seismic" geohistory analyses of basins can be carried out by backstripping the sedimentary fill through time.

Contrary to the conclusions of others, Hallam (1984) for example, we believe that the data are available in the public domain to test Vail et al.'s (1977) concepts. This belief is substantiated by the record, since seismic and well data sets are available from the Norwegian Oil Directorate for Norwegian waters, from the Bureau of Mineral Resources in Canberra for Australian waters, from the U.S. Government for the National Petroleum Reserve of Alaska, from the AAPG for the East Coast of USA (Buffler et al. 1978), and the Gulf Coast (Watkins et al., 1976), and are routinely handed out at AAPG seismic stratigraphy schools. Using these sets most of the ideas suggested by Vail et al. (1977) can be examined. In fact, Thorne and Watts (1984) use just such data to challenge Vail et al. (1977) and show that some of their concepts are not always valid.

The sedimentary record as a means of determining the magnitude of variations in eustasy.

Paleobathymetric markers tied to old strand-line positions are used in attempts to estimate the magnitude of excursions in eustasy. These markers include sedimentary structures that indicate the position of the high water mark in shoaling cycles (old beach lines, notches in old cliffs, etc.), and fossil indicators of paleobathymetry like benthic organisms, algal stromatolites, burrows, coral reef terraces, peats etc.

The relationship of eustasy to sedimentary cycles has been recognized in reviews by Barrell (1917), Wanless and Shepard (1936) and Wells (1960), and stratigraphers often estimate the size of relative sea-level excursions by measuring the thickness of sedimentary cycles in shelf sequences. For instance Busch (1983) correlated shoaling upward cycles or PAC's (punctuated aggradation cycles) in the Devonian Manlius Formation of central New York, and related them to sea-level events. He correlated the high stand cycles as identified by the upper limit of the vertical burrows or the lower limit of algal laminites within the cycles. Busch recognized three cycles which have approximately the same thickness, 3.7 ft., 3.3 ft. and 2.5 ft., respectively, at several localities, suggesting that the relative sea level had changed by this amount at these locations. Busch ignored the effect of compaction so these values may in fact record less than the actual magnitude of relative sea-level change. Busch noted that the transgressive surface, unlike the maximum high sea-level surface, climbs stratigraphically in a seaward direction. This system of estimating magnitude of sea-level excursions is obviously dependent on three *assumptions*: (1) that these cycles are a result of an eustatic dictator; (2) that each of these localities have the same tectonic history; and (3) that this tectonic effect can be accurately modelled.

In another paper, Beukes (1977) measured sea level in a study of a mix of siliciclastic and carbonate sediments from the Transvaal Super Group, a Precambrian succession from the northern Cape Province of South Africa. He estimated paleofluctuations in sea level by first assuming that the thickness of the intertidal units corresponded to the average paleotidal range. As he pointed out, the tidal flats cannot prograde without the subtidal platform surface being infilled up to the average low water mark. He felt that the thickness of the subtidal units is a measure of the water depth, but that the transgressions that he recognized in the stratigraphic column are the result of relative sea-level changes responding to tectonism. In other words, in contrast to

Busch (1983), he used the sediment thickness within his cycles to model the size of local sea-level events by *assuming* eustasy is not important but tectonism is.

McKerrow (1979), studying Ordovician and Silurian changes in sea level, used brachiopods and other benthic organisms and mapped the distribution of cycles and their paleo-water depths. He recognized that he must be seeing some of the effects of eustatic sea-level changes, but made no claim that the relative changes in sea level that he had mapped were a true measure of the size of these excursions. Presumably this is because he recognized that local changes in depth are also the product of local tectonism. Other papers by Weimer (1984), Kauffman (1977), Seiglie and Baker (1984), Seiglie and Moussa (1984), and Harris et al. (1984) take similar approaches and, while recognizing a eustatic signal, do not neglect the importance of local tectonism in producing the accommodation for the sedimentary section.

The general philosophy of the use of reef terraces, peats, cliff notches and paleo-bathymetric markers is the same as in the papers just cited. They all require assumptions either about the tectonic behavior of the depositional setting, and/or eustasy and/or sedimentation, so the magnitude of the sea-level excursion is dependent on an assumed model, which cannot be proven independently.

The use of backstripped subsidence to determine the magnitude of excursions of eustasy

(A) *Differences between crustal subsidence and thermo-tectonic curves.* Hardenbol et al. (1981) note that (1) the eustatic curves of Vail and Hardenbol (1979) and Vail and Todd (1981) are based on estimates of "changes in coastal onlap and from paleontologic studies", and that (2) the magnitude of the low frequency eustatic events can be assessed by measuring the difference between crustal subsidence curves calculated from wells and the theoretical thermo-tectonic subsidence curves postulated for that location using the approach outlined in Royden et al. (1980). Similarly Hallam (1963) proposed the possibility of measuring sea-level excursions on the basis of assumed rates of subsidence of Pacific guyots.

Essentially these crustal subsidence curves are obtained for a well by (1) determining its burial path from the datum of present-day sea-level (Fig. 5) (the geohistory plot of Van Hinte, 1978 and then (2) using paleobathymetry as a datum, removing the effects of compaction and the isostatic effect of sediment and water weight on the crust after the manner of Watts and Steckler (1979) using Airy's (1885) concept of isostacy as modified by Bomford (1971). Thus basement subsidence is estimated by compensating for the influence of sedimentation but ignoring the effect of sea-level fluctuations on this subsidence (Fig. 6).

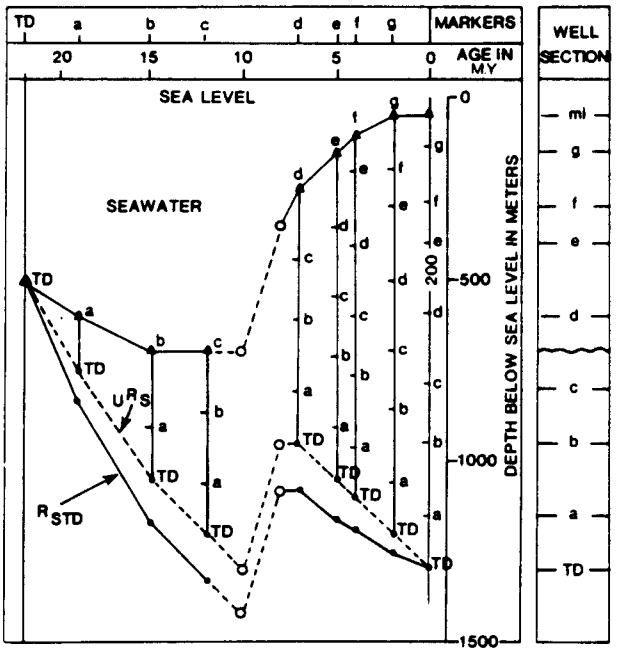

Fig. 5. Geohistory diagram for hypothetical well (after Van Hinte, 1978). Upper curve shows paleo-waterdepth at this locality. The dashed lower curve *uRs* is the uncorrected burial path of TD through time, measured cumulatively from the water/sediment interface; the solid line lower curve R_{STD} is the corrected burial path of TD which incorporates the progressive compaction of the overlying sediment as TD is buried.

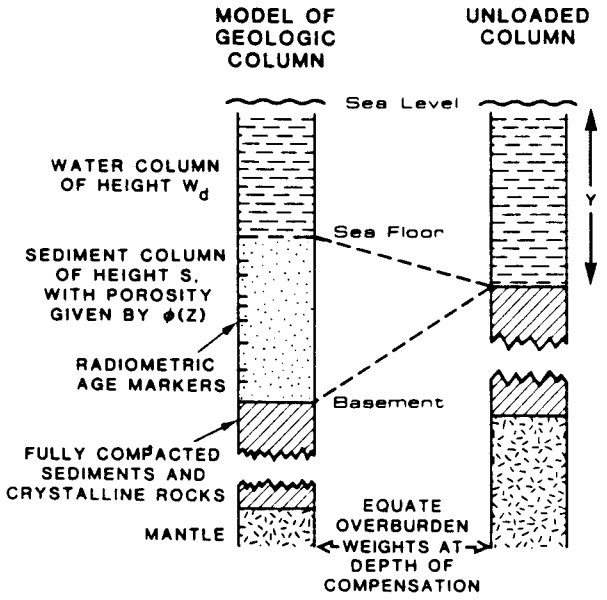

Fig. 6. Watts and Steckler's (1979) backstripping diagram.

In the calculations which are made, the total thickness of the sedimentary column above the basement at a given geologic time is commonly not available, and reconstructions are forced to use data from that part of the column penetrated by the bore hole. A consistent prediction of depth to basement may be achieved by extrapolating the porosity function ϕ below the total depth of the well to that depth at which the rocks are believed to be fully compacted. For instance Guidish et al. (1984) used a model in which porosity decreases exponentially with depth, and defined "effective basement" to be at the depth at which the sediment has a calculated porosity of 1%, when all sediments down to the total depth of the well have been backstripped. Thus in this case, "effective basement" always has a porosity less than or equal to 1%.

Lack of information about sedimentary formations below this total depth results in an uncertainty in the decompaction of the sedimentary column during the backstripping calculation. This in turn yields an uncertainty in the estimate of basement subsidence, compensated for sedimentation. However, model calculations show (Guidish et al., 1984) that this effect typically changes basement subsidence integrated over the total depositional time, by less than about 70 m (230 ft.), which is significantly less than typical basement subsidence after compensation for sedimentation.

Results obtained from the burial history calculation are illustrated in Fig. 7, which shows the reconstructed depositional history and basement subsidence curve of a sample North Sea well. These basement subsidence curves are then compared to thermo-tectonic curves and the difference between them is used to determine the size of the sea-level excursion.

However, hypothetical thermo-tectonic curves differ from author to author. For instance, McKenzie (1978) models subsidence

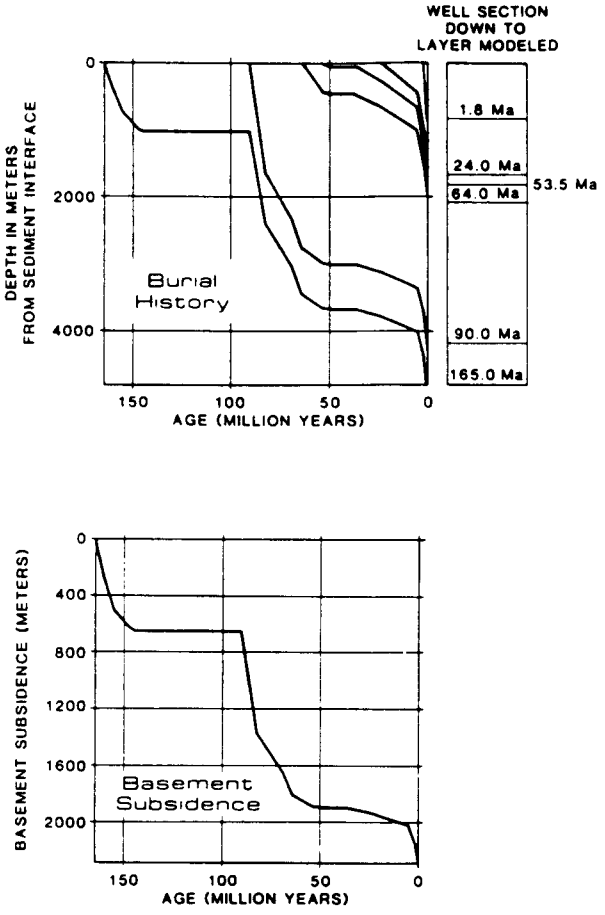

Fig. 7. Burial history of North Sea well plus crustal subsidence.

curves assuming that when rifting occurs the continental lithosphere stretches rapidly horizontally and thins the lithosphere in a predictable way. In response, the hot asthenosphere comes closer to the earth's surface but then cools conductively and predictably, causing subsidence until thermal equilibrium is reached.

In McKenzie's model the lithosphere is assumed to be a single slab in isostatic equilibrium at all times, with a constant temperature at its base. The surface of the continent is taken to be at, or below, sea-level so that water hypothetically occupies the entire volume created by subsidence because the contribution of sediment loading to overall subsidence is removed. Contributions from radioactivity of crustal rocks are ignored and two-dimensional effects are neglected entirely. The equations for this model and the physical parameters used are given in McKenzie (1978).

Hellinger and Sclater (1983) have a more complex model which uses many of the assumptions of McKenzie (1978) but involves modelling the stretching and thinning of two layers instead of one. As before isostatic compensation is maintained by the upwelling of the hot asthenosphere, which then cools and subsides until thermal equilibrium is reached. The thermo-tectonic subsidence curve produced differs from that of McKenzie's (1978) model, and by significant amounts as the parameters are varied.

In contrast the large-scale dike intrusion model of Royden et al. (1980) is constructed by assuming hot material from the asthenosphere intrudes into the continental lithosphere through a series of vertical dikes with a frequency of intrusions ranging from 5 to 50 + per kilometer. Whatever the spacing of the dikes, the thermal effect of intrusions is assumed to have equilibrated horizontally within a million years, allowing Royden et al. to neglect the horizontal component of heat conduction and consider this effect as only a simple one-dimensional problem. They assume the intruding dikes have specific thermal properties and can be modelled such that the crust subsides predictably in proportion to the fraction of the lithosphere composed of intruded dike material and its rate of cooling.

Models have also been developed by Falvey (1974), Nunn et al. (1984) and Beaumont (1981). Each model is different and was developed to find ways around weaknesses in other models. If we are to measure the difference between crustal subsidence derived from a well and thermo-tectonic subsidence, then, because the subsidence curves predicted by McKenzie (1978), Royden et al. (1980), Hellinger and Sclater (1983), and Falvey (1974) are so different, we are forced to choose one. Once we do, the difference between the crustal subsidence curve derived from a well and the arbitrarily chosen thermo-tectonic subsidence curve is given by a least-square difference system. This in turn leads to an estimate of the size of the sea-level excursion.

The results of such a calculation are given in Hardenbol et al. (1981), where they choose the Royden et al. (1980) model and apply it to an example from northwest Africa. They go on to state "the stratigraphic resolution of these changes rarely allows exact quantification of their magnitude, but a minimum rate of change of sea level can often be determined". Even though Hardenbol et al. (1981) only consider low-frequency events, it is our opinion that the assumption of a smooth model-dependent thermo-tectonic subsidence curve may be unwarranted. Despite obvious basin-to-basin correlation of lithostratigraphic units, many of the high-frequency perturbations seen on crustal subsidence curves may be tectonic in origin; this has not been established but it has been assumed. Also the fact that the parameters chosen for the Royden et al. (1980) subsidence curves provide a model with a good fit to the crustal backstripped curves does not mean that this model is correct, for the parameters are chosen to give a minimum least-squares mismatch to the crustal curve.

The error limits to this system are not estimated by the various authors but from

crustal subsidence calculations of Guidish et al. (1984) are sizeable. They are related not only to the constants used in the different models, but also to the compaction history during subsidence, to the flexural behavior of the crust, and to the model chosen to describe the thermo-tectonic behavior.

(B) *Stacked and averaged crustal subsidence curves.* Guidish et al. (1984) stacked and then averaged crustal subsidence curves to determine the occurrence and magnitude of eustatic events. Their global average rate of basement subsidence (Fig. 8) has little similarity in detail to Vail's eustatic curves. This difference suggests that high-frequency tectonic movements are reflected more distinctly in crustal subsidence curves than are eustatic events seen on the Vail onlap charts because the sea-level excursions with a magnitude of less than 90 m (300 ft.) are too small to significantly affect the crustal subsidence. Even if the crust did respond to the higher-frequency sea-level events, we could at best recognize their occurrence but not measure their size using crustal subsidence curves. This is because the limits to this system are related to assuming: (1) an equilibrium isostatic burial history; (2) a model of isostatic and flexural response to sediment and water weight; (3) a model of sediment compaction below the base of well information; and (4) that there is no stacking "error" produced by the problem of averaging. It would seem that once again we have a system that cannot determine the exact magnitude of eustatic changes.

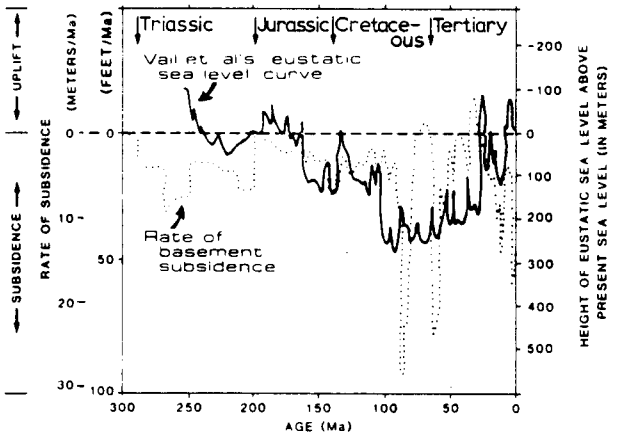

Fig. 8. Comparison of global average rate of basement subsidence and Vail et al.'s (1977) eustatic sea level curve (after Guidish et al., 1984).

Determinations of the magnitude of excursions in eustasy from isotope ratios and coral reef terraces associated with Pleistocene glacial stages

Fillon (1984) provides a very complete review of continental and marine Pleistocene stratigraphy and of how the two can be correlated and tied to eustasy. As he points out, Agassiz (1840) probably inspired geologists to begin looking at the Pleistocene in terms of glaciation. Since then geologists have recognized a series of different major and minor glaciations through the Pleistocene and have been using three principal geological sources to unravel Pleistocene stratigraphy and, in particular, the response to glacio-eustatic events. These are the terrestrial tills and interglacial sediments dated by ^{14}C and K/Ar; isotopic records from marine benthic and planktonic microfossils dated by paleomagnetic stratigraphy; and geomorphologic evidence of sea-levels based on U/Th-dated corals and ^{14}C-dated, in place, peats (Fillon and Williams, 1983).

Variations in $^{18}O/^{16}O$ ratios derived from planktonic microfossils from the deep sea can be dated and have been related to glacial eustatic events (Broecker and Van Donk, 1970; Shackleton and Opdyke, 1973; Fillon and Williams, 1983, among others). Similarly Mesolella et al. (1969), Steinen et al. (1973) and Matthews (1984a) have shown that changes in eustasy are recorded in coral reef terraces around Barbados during its tectonic uplift in the Pleistocene. These terraces were dated using the U/Th method. Evidence for the same eustatic events can be seen in reef terraces dated by U/Th in New Guinea (Bloom et al., 1974; Chappel, 1974) and Indonesia (Chappel and Veeh, 1978).

The exact causes of the Pleistocene glacial

events are unknown but can probably be ascribed to fluctuations in the distribution of solar radiation received at the Northern and the Southern Hemisphere through time, as controlled by the periodic change in the tilt of the earth's axis every 41,000 years, the precession of the equinoxes every 26,000 years and the changes in eccentricity of the earth's orbit every 90,000 years (Milankovitch 1941). Broecker (1966) and Berger (1976, 1978) modified the original relationships described by Milankovitch (1941) to emphasize the effect of precession on solar radiation. Ruddiman and McIntyre (1981) and Fillon and Williams (1983) used the Milankovitch relationships to model ice sheet formation over continental land masses and in the Arctic Ocean as well as to account for the isotopic changes in the deep sea $\delta^{18}O$ record.

Moore (1982) compiled a Late Pleistocene eustatic sea-level curve, showing sea-level change dimensions through time, based on radiometric dating of coral reef terraces in Barbados (Mesolella et al., 1969), the Far East (Chappell, 1974; Chappell and Veeh, 1978) and several other locations (Fig. 9). The size of the sea-level excursions is dependent on assuming that one of the events, that at 125,000 years B.P., was 2 to 10 m above present sea level and that the rate of tectonic uplift was constant for the geographic location of this datum between 125,000 years B.P. and today. Supporting evidence that the 125,000 BP sea level was close to that of today can be seen in the oxygen isotopic values from sediments of this age, which are close to those of today (Shackleton and Opdyke, 1973; Fairbanks and Matthews, 1978). However, as was so aptly pointed out by Ward (in Ward and Chappell, 1975), it is impossible to determine the size of the tectonic movement; to do so the size of the sea-level excursions must be known beforehand. Thus, while the dated coral terrace positions are signals produced by the eustatic events, this signal cannot be used to determine more than the relative size of the sea-level events because a model of tectonic behavior must be assumed.

Different problems are faced if we try to

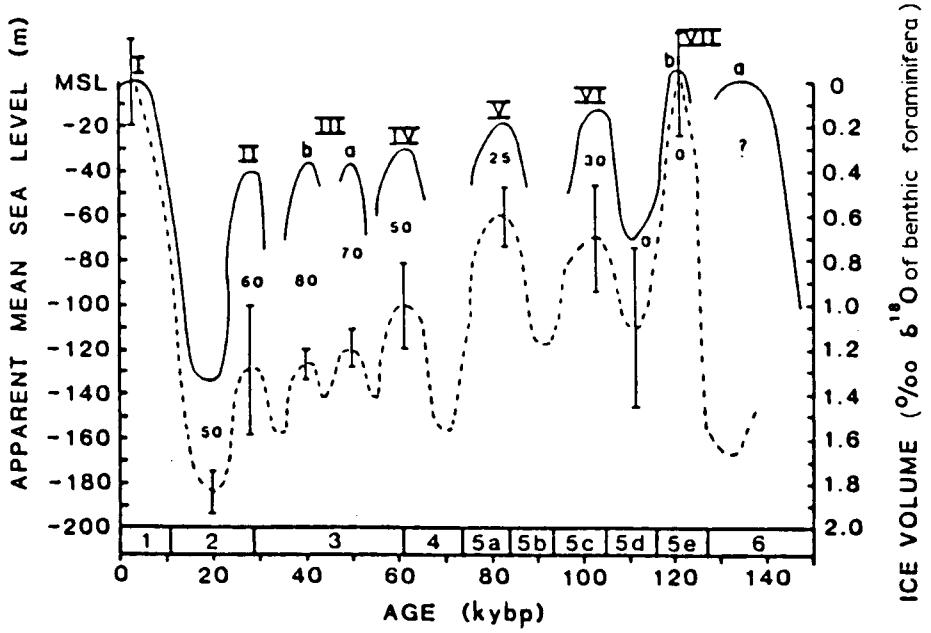

Fig. 9. Late Pleistocene eustatic sea level curves, showing sea level change dimensions through time, based on radiometric dating of coral reef terrace in Barbados (Mesolella et al., 1969), the Far East (Chappell, 1974; Chappell and Veeh, 1978) and several other locations (after Moore 1982) (solid line); and on benthic "ice volume" $\delta^{18}O$ records for the major ocean basins (Fillon and Williams, 1983) (dashed line).

determine the size of sea-level excursions from $\delta^{18}O$ variations from planktonic microfossils in deep-sea cores. Fillon and Williams (1983) show two curves for the size of sea-level excursion (Fig. 9): one from dated coral reef terraces and the other from $\delta^{18}O$. The two curves have the same frequency of signal but the amplitude of the events is different. Broecker and Van Donk (1970) were among the first to argue that sea-level position, ice volume and $\delta^{18}O$ change are related. Shackleton and Opdyke (1973) assumed that a change of 0.1‰ in $\delta^{18}O$ was equivalent to a 10-m sea-level change and produced a glacio-eustatic sea-level curve that matched that of Mesolella et al. (1969). Fairbanks and Matthews (1978) and Aharon (1983) later confirmed this relationship using the $\delta^{18}O$ from dated coral terraces. Since then Williams et al. (1981) and Fillon and Williams (1984) have examined this relationship more closely. The problem is to predict the volume of sea ice versus continental ice, and to know how much ^{18}O is trapped in the different ice bodies. Fillon and Williams (1984) produce figures that match the original generalization of Shackleton and Opdyke (1973). They claim this comes from three independent systems and it is not model-dependent. But because the results match those derived from reef terrace dating and assumed tectonic uplift models, does not prove they are correct. The dimensions of the variables involved can only be guessed at and certainly not measured (such as the rate of tectonic uplift over the last 125,000 yrs.). As it is, even if we knew the ice volume involved we would not be able to predict the isostatic response of the crust to the changes in weight of sea water since the crustal flexural properties change from one setting to the next (Walcott, 1970), and also presumably with time.

Chappell and Shackleton (1986) tie a detailed sea-level curve (derived from the Huon Peninsula of New Guinea using reef terraces and an assumed rate of tectonic uplift) to the ^{18}O record of a deep Pacific core. They are able to make excellent correlations between events but ascribe differences in the amplitude of the oxygen signal to differences in ocean temperature. Again nothing can be proved though plausible models are presented.

So the bottom line is we have a number of independent signals that sea-level excursions took place: (1) glaciological and morphological evidence; (2) deep-sea planktonic microfossils, coral, and mollusc $\delta^{18}O$ records; (3) coral terraces from a number of different locations; and (4) meltwater effects. We can estimate the relative size of these excursions, which is useful stratigraphic information, but we cannot place an exact figure on these values.

On the basis of the hypothesis that glacio-eustatic fluctuations are not confined to the Late Tertiary and Pleistocene, Matthews (1984a, b) goes further and suggests use of the oxygen isotope record in identifying and measuring the relative magnitude of excursions in eustasy back at least 100 My. However, while Matthews will probably identify the signals of sea-level this way he will not be able to put any accurate dimensions to them. Nevertheless this approach does offer hope in separating the *relative* size of sea-level events recognized using the onlap technique.

Simulation of continental margin sedimentation in response to crustal subsidence, eustatic change and sediment accumulation rates

Our intrinsic dissatisfaction with previously discussed systems led us to develop a forward (in time) model to handle eustasy, tectonics and sedimentation. The ultimate goal was to determine the sizes of the different variables needed to produce the sedimentary geometries observed within given basins by inverting the forward model.

Here we describe a means of simulating marine clastic deposition, independent of the alluvial wedge. First we deal briefly with the sequential simulation of geologic processes such as deposition, compaction and subsidence, and the required inputs. The second

part describes sources of data for input to the simulation. The last part evaluates the significance of the simulation with respect to our current understanding of shelf sedimentation and describes the simulation outputs. Appendix I describes the details of how deposition, compaction, and subsidence are handled.

A simple system of modelling was developed, designed to generate a two-dimensional representation of the sediment geometry that can be observed on dip-trending seismic lines that cross buried shelf margins (Fig. 10a). The geometries seen on seismic lines are the result of the interaction of eustasy, of sedimentation, and rates and directions of tectonic movement. Our simulation varies sedimentation, subsidence, and position of eustatic change and plots the resulting geometries. If a favorable match between the simulation plot and the seismic cross-section could be seen, then some specific statements could be made concerning sediment accumulation rates, subsidence rates, and sea-level changes. These data, in turn, could then be applied to the lithofacies geometries in basins. As with all the other methods of determining sea-level this one too makes assumptions as to the size of the variables.

The simulation is based on the concept that important gross features of the depositional geometry are controlled by macroprocesses such as variations in eustasy, crustal subsidence, compaction and sediment deposi-

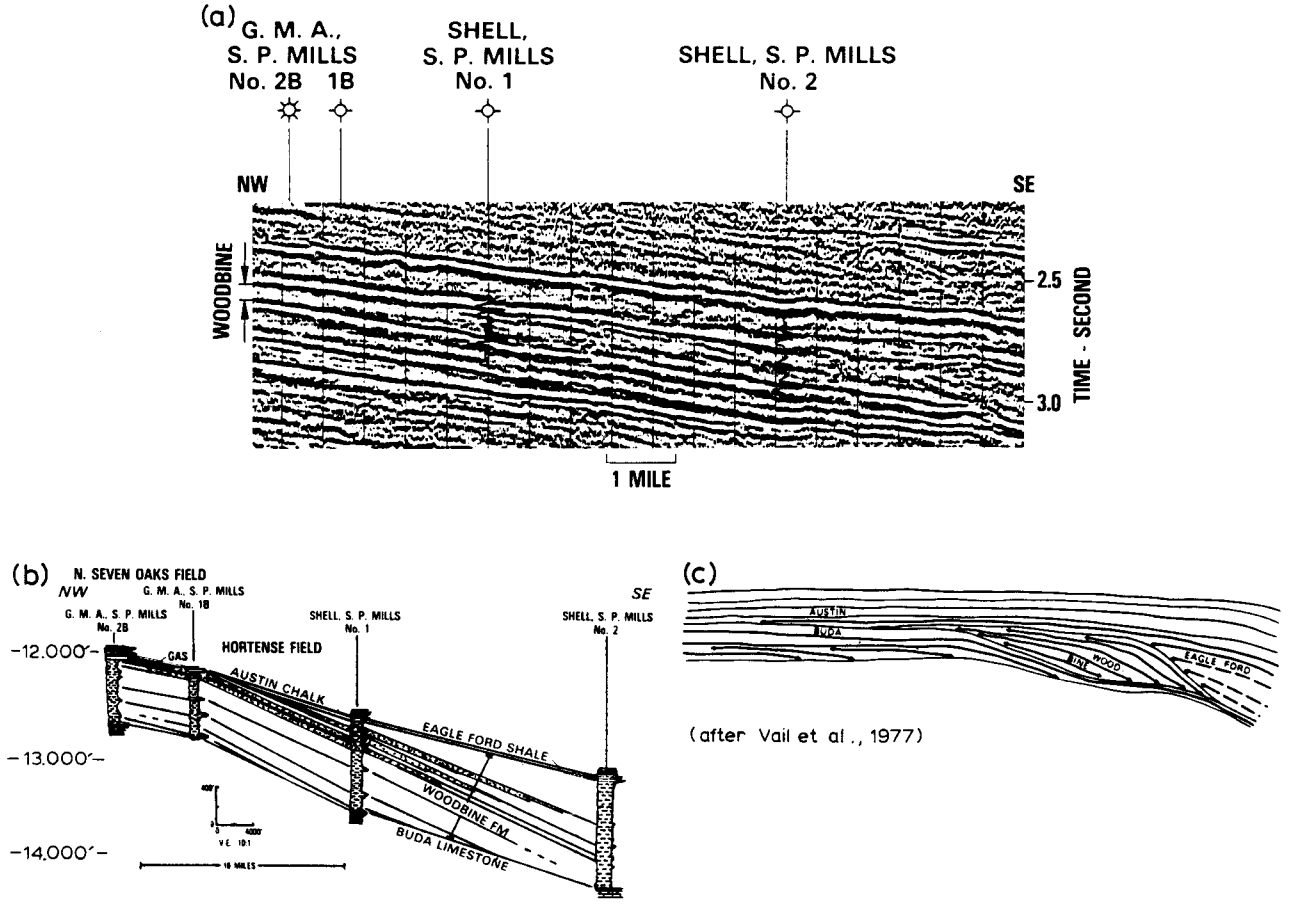

Fig. 10. a) Seismic cross-section through the Woodbine delta, Polk Co. Texas.
b) Electric log cross-section showing distribution and geometry of Woodbine delta, sandstone beds, Polk Co. Texas.
c) Diagrammatic interpretation of the Figures 10a and 10b. All after Vail et al., 1977.

tion, precisely the processes which are needed to interpret the stratigraphy of seismic sections. No attempt is made to actually simulate the physical processes involved. Rather, we attempt to reproduce the sedimentary geometries, which are the results of such processes, averaged over long periods of time.

We simulate the deposition over fixed time intervals which we define as sediment triangles of specified length and thickness (Fig. 11B). The distribution of these packages for each time interval is controlled by: (1) the configuration of the original depositional surface (Fig. 11A); (2) the level of the sea relative to that surface (Fig. 11D); (3) the quantity and distribution of sediment (shale and/or sand) deposited during that time interval (Fig. 11B); (4) the subsidence behavior of the depositional surface (including hinged tectonic or thermal subsidence, isostatic loading, and sediment compaction in response to dewatering) (Fig. 11C).

The simulation includes functions that allow the sediment to build to sea level, after which erosion and bypass take place.

The simulation inputs, such as variation in eustasy with time, are described in the section that follows. Each depositional surface is defined, for a given time, by an array corresponding to the vertical position of the surface between evenly spaced horizontal points, giving all surfaces a staircase-like appearance (Fig. 12). Fig. 13 schematically illustrates the depositional geometry after five time steps. The staircase-effect seen in the figure is not visible in the output because of the large number of horizontal points. The basic sequence of processes followed in each time step is as follows.

(1) Locate the point of greatest onlap (POGO), i.e. the intersection of sea-level and the highest sediment surface (Fig. 12).

(2) Erode between the point of landward-most previous sediment deposition, and POGO (Fig. 12).

(3) Deposit sediments, including those eroded in step (2), and those to be deposited for that time step.

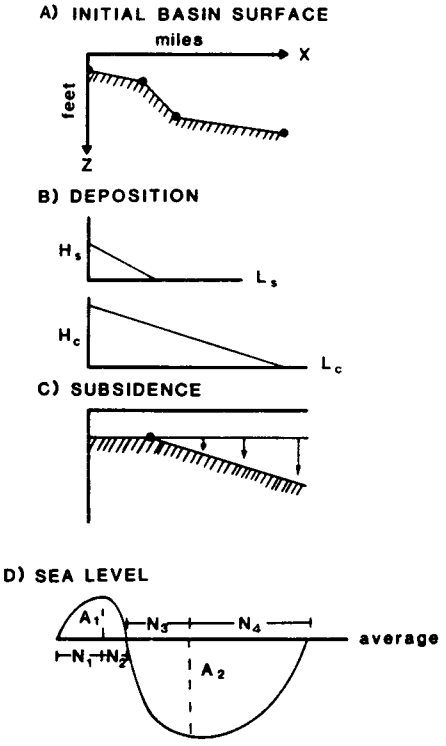

Fig. 11. Definition of the size of the input parameters used in the graphic simulation.

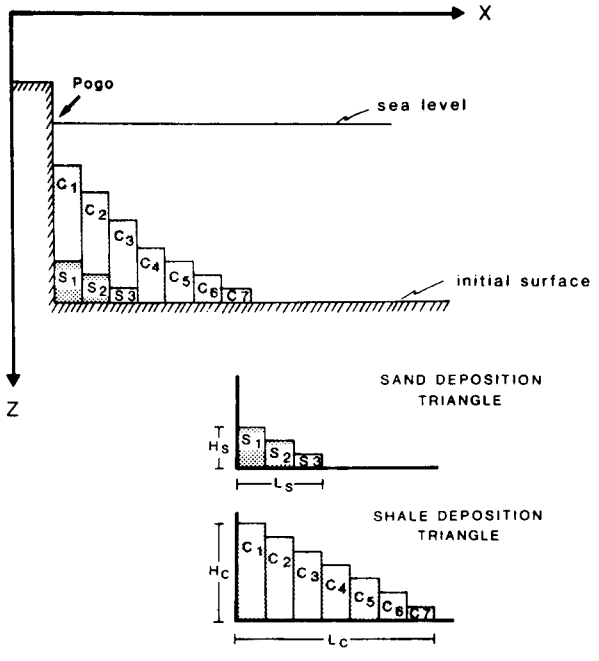

Fig. 12. Depositional surface defined by an array of evenly spaced horizontal points, giving surface a staircase-like appearance.

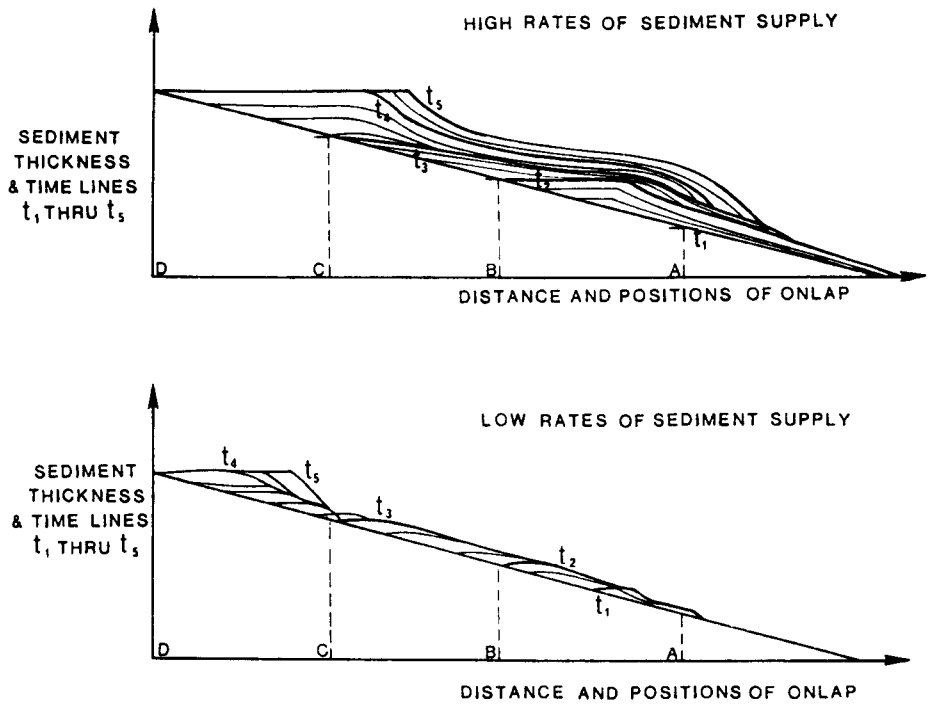

Fig. 13. Cartoon of depositional geometry after five time steps.

(4) Compact all sediment layers according to the weight of overlying rock.

(5) Subside all surfaces in response to a fixed linear tectonic dependence about a hinge point and the isostatic accommodation due to sediment loading and change in water depth. The isostatic accommodation is assumed to be perfectly elastic and for the crustal parameters we use Bomford (1971).

This sequence of erosion, deposition, compaction and subsidence is carried out for each time step. Deposition involves the creation of new surfaces at the same height as, or above, the highest previous surface. Both erosion and compaction involve reduction in the thickness of layers. Tectonic subsidence causes all surfaces to drop vertically at the same rate at a given horizontal position (Fig. 11C).

Detailed descriptions of erosion deposition, compaction, and subsidence as well as the simulation inputs and outputs can be found in Appendix I. Fig. 14 provides a simplified flow chart of the simulation.

Results of the simulation. Our purpose was to simulate marine clastic deposition alone, ignoring the alluvial wedge landward, and so reproduce the gross sedimentary geometries of the marine sediments of this setting, thus showing the location of sand-prone and shale-prone portions of the section (Fig. 15). We appreciate that without the alluvial plain our simulation is less than perfect and we are

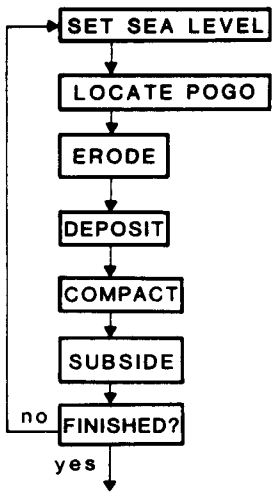

Fig. 14. Simplified flow chart of simulation.

working on this lacuna (Helland-Hansen et al., 1986). However, we think the present simulation results are significant and informative. The areas between dark lines represent the sediment deposited during equal time intervals. The proportion of shale and sand within the time step is displayed in the following way. The area immediately below the dark lines represents the shale portion of the sediment, and the area below the light lines represents the sand portion. Individual sand and shale bodies, such as point bars, filled channels, or deltas, are not specifically identified, although areas where sand or shale bodies are likely to occur are shown. The primary objective of this output is to aid in the interpretation of seismic data by simulating the general, rather than specific, depositional history of the rock sequence. In particular the simulation can be utilized to help identify probable zones of good hydrocarbon source rocks and hydrocarbon reservoir seals (shale-prone areas), and the general region in which potential stratigraphic traps for hydrocarbons (pinch-outs of sand-prone areas within and/or beneath shale-prone areas) may occur.

Figs. 15 and 16 show the progressive evolution of the shelf and basin margin geometry with a small element of hinged subsidence. At Stage 1 the progressive onlap of the shelf in response to a relative sea-level rise is seen which is a function of the interplay between rate of eustatic change, rate of subsidence, and rate of sediment accumulation; in Stages 2 and 3 we see toplapping progradation in which sea-level fall is not rapid enough to drop the coastal sedimentary wedge below the shelf margin. In Stage 4 we see the effect of a relative sea-level rise and the onlapping sedimentary wedges. At each stage the graphic output is the product of the interplay between eustasy, subsidence, sediment supply and compaction rather than eustasy alone. One of the interesting responses we see in the simulation is the effect of the isostatic response of the crust to loading by sediment and water. In the first stage the crust is bowed down, close to the shore, while at the basin margin, the crust develops a positive ridge through a lesser rate of subsidence. In the third and fourth stages, the crust is bowed down seaward of this earlier positive ridge. The reason

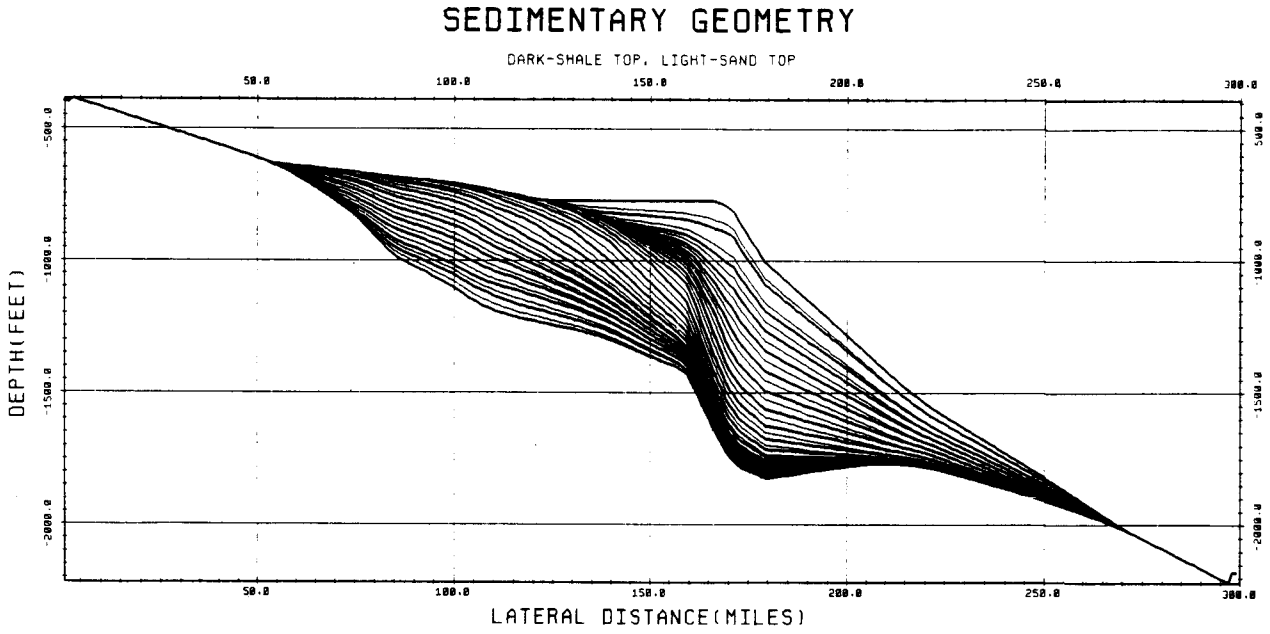

Fig. 15. Cross-section of sedimentary geometry produced by simulation of eustasy, compaction, tectonic movement, isostacy and sediment fill assuming no alluvial wedge landward and sediment fill to sea level.

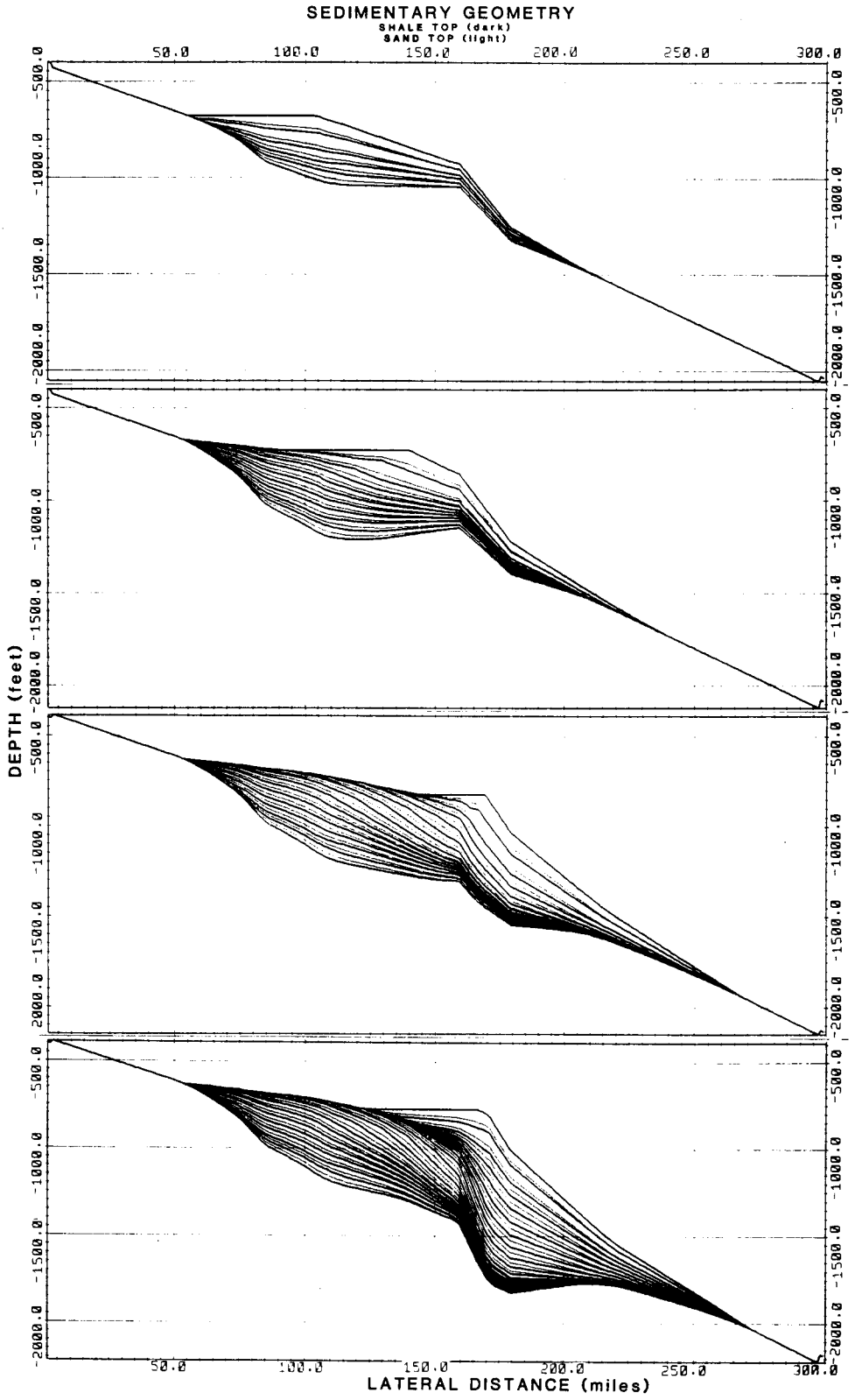

Fig. 16. Five steps involved in sediment fill to produce geometry of Fig. 15.

for this is that sediment accommodation is reduced on the shelf and the sediment now occupies space to seaward causing downwarping here. The resulting "basement" geometry is a product of sediment weight alone, assuming a perfect elastic Airy response of the crust.

Fig. 17 shows two curves. The lower line plots the changes in eustasy input to the program, added to tectonic subsidence and compaction per time step. This curve has a maximum excursion of 46 m (150 ft.). Thus the lower line is determined from the difference in height of onlapped sediment per time step. Also plotted is a modified Vail aggradational curve which does not include the alluvial plain and which has a maximum excursion of 85 m (280 ft.). This upper line is a plot of the difference in height of onlapped sediment per time step measured from the final geometry of the simulation after the deposition of the whole sedimentary package. This latter uses the same criteria as outlined by Vail et al. (1977). Thus, the upper aggradation line, the Vail et al. (1977) sea-level excursion (or coastal onlap curve) determined by the simulation shows a two-fold exaggeration over the lower. In the Vail et al. aggradation the relative rise in sea level appears much larger than the fall. We expect this magnification and distortion would be even larger if the alluvial-plain sediments were added. This magnification effect possibly explains why the sea-level excursions of Vail et al. are so large and yet the crustal response seen by Guidish et al. (1984) is so small. Using the simulation results it would appear that when small sea-level excursions are input, not only do they have a marked effect on the sedimentary response, but compaction and tectonic movement exaggerate the size of the excursion when one tries to measure it either from the final geometry of the simulation and (presumably) from seismic cross-sections by the method of Vail et al. (1977).

Fig. 18 shows the simulated positions of POGO (the point of maximum landward encroachment of coastal onlap), the shelf break

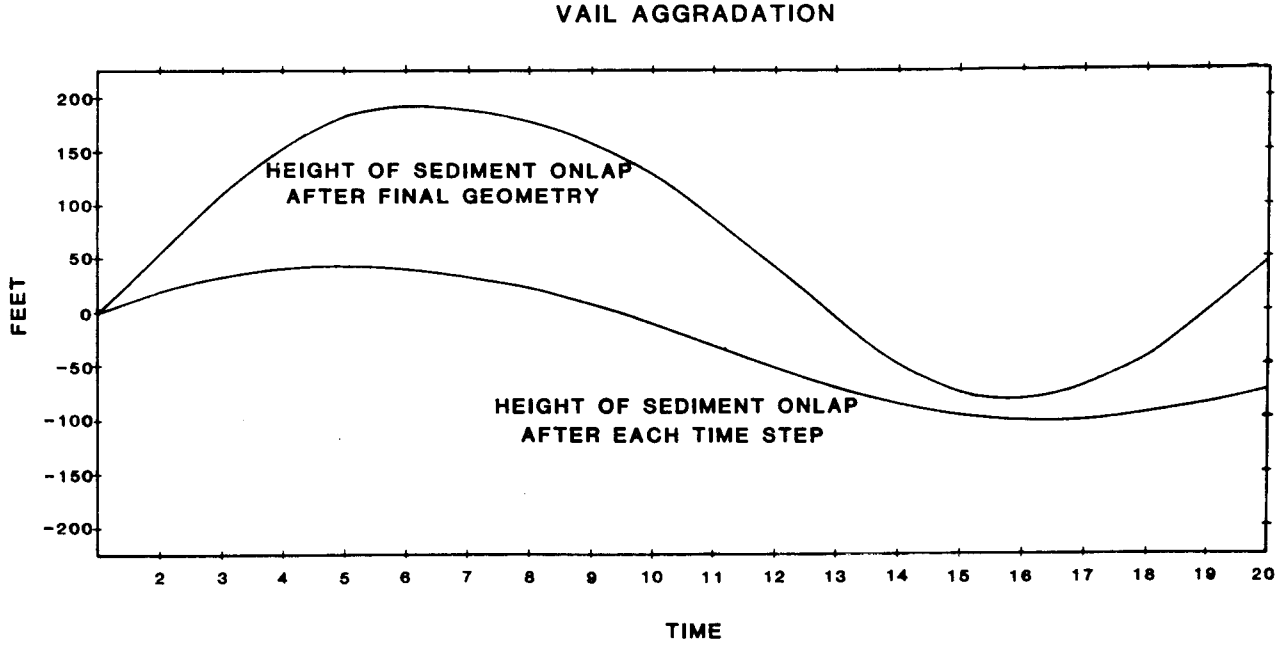

Fig. 17. Vail aggradation curve (plot of difference in height of onlapped sediment per time step) measured after final geometry (top line) versus variation in eustasy coupled to tectonic subsidence and compaction after each time step (bottom line).

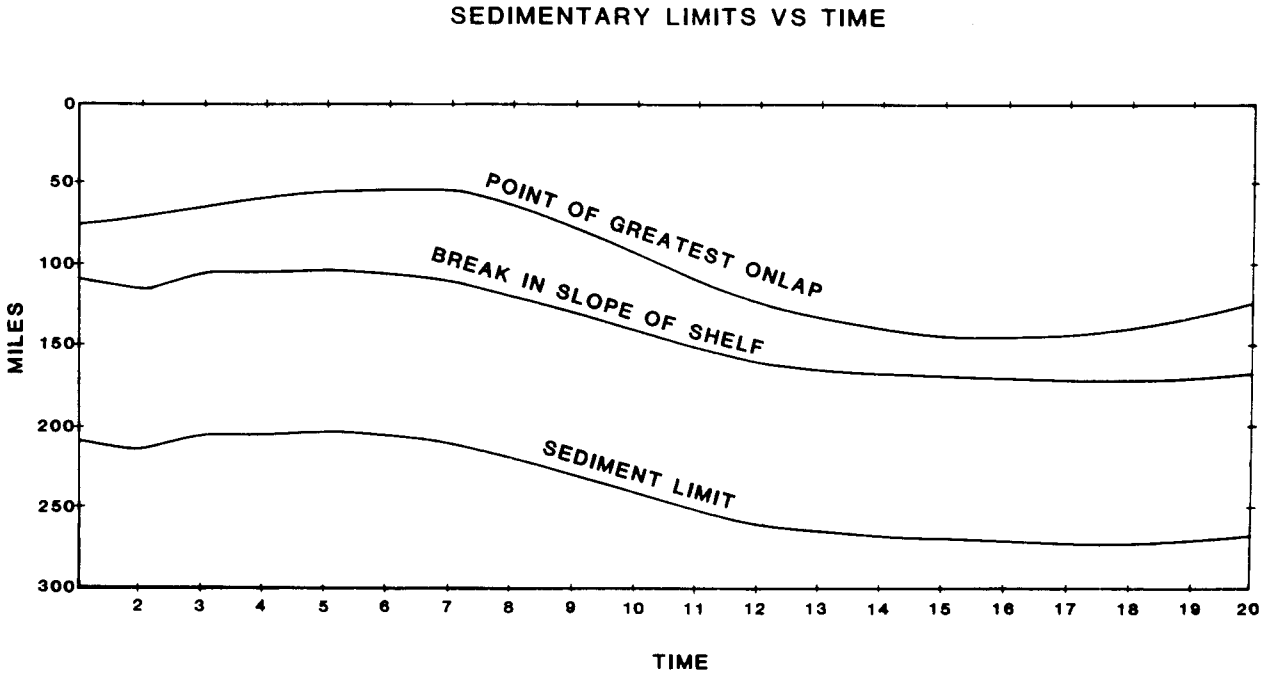

Fig. 18. Position of POGO, (top line) shelf break, (middle line) and most basinward position of sediment wedge (bottom line).

and the furthest basinward position of the sediment wedge through time. The sinusoidal shape of these curves and of the coastal onlap curve owe their shape to the sea-level variation, as well as to the fact that we are not modelling the alluvial plain sediments which, as Hardenbol et al. (1981) point out, are responsible for the saw-tooth appearance of their "coastal" or sediment onlap curves. Thus a major element yet to be added to the simulation is the alluvial wedge that onlaps landward of the coastline (Fig. 4) (Helland-Hansen et al., 1986). Nevertheless, the simulation gives a general sense of the response to sedimentation, sea-level and tectonism in the offshore marine and coastal sediments.

A systematic test of the simulation's reliability and its effectiveness as an aid to the interpretation of sedimentary stratigraphy has yet to be evaluated. Once we have added the alluvial wedge we plan to test the simulation in a well-studied area which provides good geologic control and to make reasonable estimates of the program inputs. Obviously such an area should lack geologic phenomena not included in the program, such as faulting, carbonate buildups, salt movement. Until that is done the applications in less known areas cannot be made with confidence.

The simulation is not difficult to use, and, if reliable data are available, sedimentary stratigraphers can use similar graphical systems to account, for instance, for the occurrence of downdip sandstone bodies. Once we add the alluvial plain sediments and test the simulation's reliability, we see the subsidence/sea-level/sedimentation simulation as an exciting, new, and useful tool for stratigraphers but not as a means of estimating the magnitude of eustatic excursions.

Later in the paper we determine that the simulation geometries would be similar for a whole variety of inputs suggesting that unique input parameters cannot be determined.

We believe the simulation can be used to produce a series of solutions which encompass the truth. It would seem to be pointless to continue arguing about which model is correct, since we probably can never establish this, but we should aim at acquiring a family

of solutions. We should look for data which may limit the solution family to a smaller set, such as discarding results that are physically impossible; and for broader purposes we should try to identify effects common to many solutions.

General summary and discussion of methods for measuring sea level

Because the magnitude of eustatic change cannot be measured directly geologists are forced to use the variety of methods listed and described through this paper. The problem is that these schemes are dependent upon some assumption about the size (amplitude, frequency, etc.) of one or more of the variables in the model.

In the case of the use of hypsometric curves and paleogeographic maps which demark the area of marine onlap across the continent, geologists are forced to assume either that the configuration of the hypsometric curve is the same in the past, or to construct an assumed curve of their own. The result is a relative sea-level curve which helps unravel stratigraphic history but does not provide measurements of the size of excursions.

With Hardenbol et al. (1981) we note that the sedimentary aggradational curves are not an accurate means of determining the size of an eustatic event either, because the measure of sedimentary aggradation is also influenced by compaction, rate and magnitude of crustal subsidence and, importantly, the extent of alluvial plain onlap; all of these latter variables are particularly difficult to determine accurately. For instance, the commonly used compaction algorithms are based on the assumption that fluid pressure is hydrostatic (Guidish et al., 1984). Clearly fluid escape is much more complex and compaction is not handled accurately by these algorithms. In the schemes that use thermo-tectonic models to predict a crustal subsidence curve to determine the size of the eustatic excursion, the result is dependent on the choice of the model used and the parameters of the model. This choice of a particular thermo-tectonic model is not grounded in fact, no matter how well and cogently the model is argued and presented. In the same way a tectonic model has to be assumed when using the height between strand-line markers like coral reef terraces, peats, and sedimentary structures to measure the magnitude of eustasy. Often it is considered that a constant rate of uplift suffices. Perhaps it does. But the point is that an assumption is being made which must be justified by data. Similarly, attempts at measuring high-frequency sea-level changes from stacked subsidence curves do not work since the crust does not respond significantly to such small sea-level events. The use of oxygen isotopes does not give a clear-cut answer either because the oxygen isotope ratio in the sea is controlled only in part by the ocean volume. Even if that portion of the isotope ratio correlatable to water volume could be established, we cannot determine the size of eustatic excursions, since we cannot accurately model the crust's flexural response to changes in ocean volume except in direction and very general magnitude. Lastly our attempts at determining the variables through numerical and graphical simulation are equally unsatisfactory because of the apparent lack of a unique solution for specific input variables.

All these methods require making basic assumptions about the size of a number of variables that cannot be measured. Exciting and imaginative concepts have been formulated but so far without unequivocal supportive evidence.

AN OUTLINE OF A SYSTEM FOR DETERMINING VARIATIONS IN EUSTASY FROM BASIN FILL UNDER ISOSTATIC BURIAL HISTORY

Having examined the schemes for estimating the magnitude of excursions in eustasy we were still no nearer to being sure that we could determine the correct size for the variables involved with each scheme. As a result we tried to see if there was a mathematically unique answer. The results are informative

and explain why we found we could not determine the size of the variables even with forward modelling (see Appendix II).

Our conclusion from Appendix II is that the entire process is very non-linear. To determine eustatic change from present-day measurements of sedimentary strata and their onlap points by inverting a forward modelling procedure would seem difficult if not impossible. And, even if a forward model could be inverted, two major problems remain.

(1) All we can deduce is *the sum of eustasy and basin motion*.

(2) We do not know where the points of *greatest* onlap are in an onlap sequence without the complete basin history, which requires: (a) complete knowledge of sedimentary fill laterally in a basin (including erosion) together with the basement response; and (b) we have to know how excess fluid present with time influences the sequence and onlap effects—since basins are not isostatically controlled for all time.

CONCLUSIONS

Geologists are haunted by Krynine's anguished cry "stratigraphy can be defined as the complete triumph of terminology over facts and common sense" (ca. 1950, John Ferm, pers. commun. 1985). Perhaps the reason some stratigraphers in their ignorance resort to terminology is that the facts or data often cannot be acquired.

Sedimentary geometries commonly seen on seismic cross-sections and in outcrop are the products of variations in rates of sediment accumulation, eustatic sea-level movement and tectonic movement. To date, the use of neither hypsometric curves, the innovative concepts of Vail and his co-workers, the paleomarkers of strand-line position, the ties to stacked crustal subsidence, the systems for measuring Pleistocene sea-level movement using either reef-terrace positions or deeper ocean oxygen-isotope ratios, or our own forward modelling presented here, provide unique and unequivocal keys to determining the size of tectonic movement, sea-level excursions or rate of sedimentation (Table II). The major conclusion from Vail's work, from our crustal subsidence work, from a forward modelling algorithm, and the formal mathematical development presented here, is that unless one variable is dependent on another two (a relationship which we do not have), at the very least two of the three processes (sediment accumulation, eustasy, tectonic subsidence) *must* be specified in order to determine the third. The relative sizes of these processes can be guessed at by modelling them from basin to basin, but absolute values remain elusive. Presumably this lack of knowledge underlies the variety of the many equally good hypotheses often invoked to account for observed sedimentary geometries. It is more than a matter of opinion that the information just is not present to decide which hypothesis represents truth.

Thus, though an *accurate* eustatic sea-level variation chart would be a boon to stratigraphers and to geologists working in frontier basin exploration in the oil industry, particularly where seismic cross-sections and occasional stratigraphic and/or wildcat well are the only data sources, such a sea-level chart cannot be made. However, when *relative* sea-level charts (combining tectonic and eustatic effects) are tied to wells, it is still possible to project sedimentary sequences related to the relative sea-level events across a basin on seismic cross-sections after the manner of Vail et al. (1977) and Hallam (1981). Possibly, and arguably, the best *relative* (tectono-eustatic) sea-level chart to construct would use a combination of sediment onlap of the continent margin, dimensioned against the oxygen isotope signal responding to continental and mountain glaciation events back to at least 100 M.y., though it is questionable whether glacial events existed back that far. Using such a chart and a simulation, a family of solutions could be produced. Then assessments can be made of the potential of finding, say, sand-prone versus shale-prone versus

TABLE II

Methods for estimating the size of eustatic sea level excursions

Method	Measured variable	Assumptions	Problems
Hypsometric	Area of continent covered by marine sediments for time interval on equal area projection measured with planimeter	The relationship between continental relief and area of continent at that elevation today is the same in the past	(1) Time interval may be too long. (2) Paleogeographic maps are inaccurate. (3) Tectonic behavior unknown. Thickness unknown.
Vail sediment onlap	(1) Distance of onlap of seismic reflectors on unconformities, perpendicular to shore (2) Height of onlap	Onlap not a product of (1) tectonic subsidence, (2) compaction, or (3) isostatic response	Cannot put dimensions on tectonic subsidence, compaction or isostatic response.
Paleobathymetric markers			
(1) Shoaling cycles	Thickness of cycle between high-watermark indicators	(1) Thickness a result of eustasy (2) Tectonic subsidence, compaction and isostacy negligible	Effects of tectonic subsidence, compaction and isostacy are unknown.
(2) Strand-line markers (Beaches, reefs, notches, peats, etc.)	Elevation above present day sea level and between markers	(1) Result of eustasy and constant rate of tectonic uplift	Tectonic uplift rate unknown. Constant behavior unknown.
Crustal subsidence curves			
(1) Divergence from thermo-tectonic curves	Difference between crustal subsidence curve for a well and predicted thermo-tectonic curve for same location	(1) Depth to average 1% porosity and/or basement (2) Compaction history (3) Isostatic response to sediment load (4) Thermotectonic model	Depth to 1% porosity and basement may not be known. Compaction history unknown. Isostatic response of crust unknown. Thermo-tectonic behavior unknown.
(2) Perturbations on stacked crustal subsidence curves	Size of perturbations from integrated stacked subsidence curves	(1) Depth to average 1% porosity, and/or basement (2) Compaction history (3) Isostatic response to sediment and water load on crust (4) Lithospheric rigidity and thermo-tectonic model	Cannot determine the assumptions.
Oxygen isotopes	$\delta^{18}O$ values	(1) Variation in δO^{18} value is a result of ocean volume (2) Isostatic response of crust to weight of water the same everywhere (3) Can estimate volume of continental ice and volume of ocean ice as function of time (4) No diagenetic effect	Cannot prove any of the assumptions.

carbonate-prone sections, an objective of so many hydrocarbon exploration companies. Models involving "relative" (tectono-eustatic) sea level will test novel hydrocarbon play concepts and initiate exploration in frontier areas.

ACKNOWLEDGEMENTS

This paper is an outgrowth from work begun at Gulf Research lab; the simulation results were previously presented at Lamont-Doherty Geological Observatory in November 1979; and the stacked subsidence research results in Guidish et al. (1984). We express our appreciation to Willard Moore and Doug Williams at the University of South Carolina who have helped us with our understanding of Pleistocene sea-level determination; to Peter Vail who, through numerous conversations, has tried to straighten out our thinking on eustasy; to Ric Busch, Timothy Cross, Jim Sadd, Ric Sarge, Larry Stoss, and Doug Williams who read and offered suggestions to improve our paper; and to Robert Ehrlich whose geologic ideas, advice and command of the English language have constantly delayed our submitting this paper. Funds used to carry out this research at the University of South Carolina were kindly provided by Chevron, Cities Service, Lytton Industries, Marathon, Norsk Hydro, Saga Petroleum, Statoil, Sun, Texaco, and Union of California.

APPENDIX I

Erosion

Erosion is simulated by stripping off rock to a constant depth between the present POGO (Fig. 11) and the landwardmost of previous POGOs at distance *XE*. The erosion depth is determined by dividing the maximum area of sediment which can be eroded per time step, by the distance *XE*.

Major constraints are placed on erosion. Only previously deposited (by the simulation) sediments above sea-level are available for erosion, i.e., no erosion into the initial surface can occur. This is because the simulation input does not define sediments below the initial surface.

The layers of sediment available for erosion, both sand (coarse) and shale (fine), are increasingly compacted with depth. Following the erosion of these variously compacted rocks to a depth D, eroded sands and shales are decompacted to their original porosity, increasing the thickness of any removed sediment $d_2 = d_1 (1-\phi_1)/(1-\phi_2)$ where d_1 is the compacted thickness, and ϕ_1 and ϕ_2 are the compacted and original porosities (the original porosities of sands and shales at deposition are 0.4 and 0.75 in the program).

The total eroded quantities of decompacted sands and shales are then added to the sand and shale already available for deposition for that particular time step.

Deposition

Following erosion, coarse (sand) and fine (shale) sediments are deposited seaward of the POGO subject to two principal constraints: the sediment functions specify the amount of each sediment to be added to the top of the last surface as a function of distance from the POGO, and the sand is deposited first, then the shale. The resultant cross-section (Fig. 15) of the sand–shale distribution represents the relative proportions of each, with distance, without providing any insight into their specific geometries, i.e., while the probability of sand bodies or percent sand at a given location can be inferred, the size and location of individual sand bodies cannot.

The thickness of deposited sediments, both sand and shale, is assumed to decrease seaward of POGO within any time step. For simplicity, the sand–shale deposition functions are triangles defined by height H and length L, both parameters specified by the user (see Fig. 12). In the figure shown, the input deposition functions do not vary with time, and the shale triangle was assumed longer than the sand triangle.

Prior to deposition, the quantities of decompacted sand and shale accumulated by erosion are added to the input deposition triangles by increasing only the height of the respective triangles but not the length. The rationale is that the distance of sediment deposition from POGO depends primarily on properties like particle size and currents rather than volume of sediment.

The sediment deposition simulated by the program consists of columns of blocks of varying thickness to which additional sand and shale blocks may be added at each time step. The sediment deposition functions are like a set of blocks of linearly decreasing height. Deposition begins by stacking first the largest sand block and then the largest shale block onto the column corresponding to POGO. Shifting seaward one column, the next largest sand and shale blocks are added and so on until the blocks run out (Fig. 12).

This simple picture is modified by two constraints. First, deposited sediment is stable over long periods

where the slope of the depositional surface is below the angle of repose. Above this critical angle, even sediments temporarily stable are assumed to be removed by sporadic turbidites or similar erosive processes. Using an input critical angle for stable deposition, the vertical drop between adjacent columns determines if deposition is allowed to occur upon a given column. If the vertical drop is more than allowed by the critical angle, the simulation skips that column without depositing, going on to the test the next column.

Second, sediment within the constraints of the model cannot be deposited above sea level. If the sand and shale blocks to be piled onto the column actually reach above sea level, the thickness of both blocks is reduced such that they just come to sea level. The relative sizes of the two blocks are reduced in proportion to the sizes by which they exceeded sea level at that position, for the time step. The sand and shale left over are added to the sediment triangles by increasing the height of the remaining triangles and not their length, i.e., the number of remaining blocks is unchanged by the increase in sediment.

Finally, the simulation tests to see if deposition has been completed, i.e., no more blocks. When deposition is completed, the program moves on to compaction.

Compaction

As with the decompaction of sediment performed in the erosion segment, compaction requires knowledge of the thickness of layers (the sediment blocks) and their present porosities, i.e., their present state of compaction. For each block, the weight of overlying blocks determines the porosity. We have, however, used empirical expressions relating porosity and depth for sands and shales.

Shale porosity is taken to vary as $\phi\alpha \ln Z$, where Z is the depth of burial. Uncompacted porosity for shale is 75% while the porosity at 10,000 ft. is about 20%. For sandstones, the void ratio, the ratio of pore space to rock space, is inversely proportional to depth. Uncompacted porosity for sands is 40% while the porosity at 10,000 ft. is about 27%. With depth, d, given in feet, porosity for shale is defined here as:

$$\phi = 0.75 - 0.06 \ln d$$

and for sands

$$\phi = 0.27a/(a + d)$$

where $a = 2.1 \cdot 10^4$ ft.

In these empirical expressions, d represents the thickness of overlying sediment. If the porosity is already less than the computed value for the depth, no compaction takes place. The latter can occur when erosion has reduced the depth of the sediment. When sediment is eroded, the remaining sediments do not decompact. Thus, when weight is again added, compaction does not occur until the new weight exceeds that previously eroded.

Subsidence

Three independent types of subsidence are included: (1) a global subsidence on the scale of the model, taken to be a constant independent of horizontal location; (2) a subsidence which increases linearly seaward of the hinge point (Fig. 11); and (3) isostatic accommodation to sediment loading and change in water depth. The first two are independent of sedimentation. The three components are summed at each horizontal position and the column or block shifted down accordingly.

The isostatic response to sediment loading is found from an equation stating that the weight of water, sediment and mantle to some fixed depth is conserved:

$$\rho_w \Delta_w + \rho_s \Delta_s - \rho_m \Delta_m = 0$$

where ρ_w, ρ_s, and ρ_m are the densities of water, sediment and mantle and Δ_w, Δ_s, and Δ_m are the changes in water, sediment and mantle thickness. The isostatic response is:

$$\Delta_m = (\rho_w/\rho_m)\Delta_w + (\rho_s/\rho_m)\Delta_s$$

The densities are known: $\rho_w = 1$ g cm^{-3}, $\rho_s \simeq 2.7$ g cm^{-3}, $\rho_m = 3.4$ g cm^{-3}, and Δ_s is the newly added sediment.

Summary of simulation inputs

The following are descriptions of the simulation inputs. As mentioned above the derivation of some of these inputs is from readily available geologic information. To run the simulation the following is required.

(1) Initial surface—defined by a set of points with linear interpolation between them; vertical units are feet; horizontal units are miles. In the example we show in the figures, the number of vertices cannot exceed 60.

(2) Horizontal range (in miles) with start and end values used in output plots.

(3) Range of time in millions of year—start and end values used in output usually determined from paleo data.

(4) Number of time steps.

(5) Stable deposition angle—assumed 2° unless changed.

(6) Max. area eroded/time step—assumed 0 unless changed.

(7) Length and height of sand and shale deposition.

(8) Global subsidence/time step which is kept 0 unless changed.

(9) Hinge point and slope of tectonic or thermal subsidence seaward from hinge point.

(10) Density of matrix rock and shale at deposition assumed to be 2.7 g cm^{-3}.

(11) Sea level variation—defined by average, initial

phase, and amplitude/half cycle and time steps per 1/4 cycle.

(12) Time steps after which geometry plots are desired.

Output plots

(1) Geometry of deposited surfaces at the end of each user's chosen time step (Fig. 15). The initial surface is plotted as a thick line. The subsequent alternations of sand and shale surfaces are shown in alternating thin and thick lines. Horizontal scale is in miles, and the vertical scale is in feet.

(2) Vail et al. (1977) aggradation versus time (Fig. 17). Vail aggradation, although carrying at least a fourfold exaggeration and some distortion, is a means of estimating sea-level variation from the rock geometry. Two curves are plotted, the thicker curve represents the true aggradation history, while the thinner curve is derived from the final geometry, simulating the estimate of sea-level variation, using Vail's method.

The technique associates the vertical change in successive POGOs with variations in sea level, although this neglects the different subsidence histories of the various POGOs with time. This even affects the true aggradation curve, since the previous POGO has always subsided somewhat between time steps, and therefore, the difference in the two POGOs includes subsidence of the first POGO with the change in sea level.

(3) Horizontal location of POGO, break-in-slope, and last point of deposition versus time (Fig. 18). The break-in-slope is defined as the last point at which sediment filled to sea level.

Suggested sources of data input for simulation

This section describes the sources of data which can be input to the simulation and Fig. 16 shows an example of this, for clastic deposition, and the resulting gross sedimentary geometries (Fig. 15).

(1) *Number of time steps*. The duration of each step is determined by the length of the simulation (as defined by the start and end times) divided by the number of time steps. To simulate accurately the sediment geometry, which results in part from sea level variations, the total time sampling must be no less than the time between maxima and minima of the sea-level oscillations with, preferably, several samples between peaks and troughs. Thus the length of a time step must be less than the minimum time between sea-level extrema and the number of time steps is just the total time desired (say 25 My, giving 25 time steps).

The length of time taken for the sea-level cycles may be determined from paleontological dating. A variety of published charts including those for the Jurassic and Cretaceous by van Hinte (1976a, b), those for the Tertiary by Vail and Hardenbol (1979), a time scale for the Phanerozoic and Archaean by Harland et al. (1982) and for North America by Palmer (1983) provide the relationship between geological ages and a chronometric time scale. An individual sea-level cycle may last anywhere from a few thousand years to 12 million years, so the length of time steps will vary according to the length of these sea-level cycles.

In our simulation, plots can be made after any time step to display sedimentary geometry (Fig. 16). After the final time step, any of the plots shown in Figs. 15, 16, 17 and 18 can be displayed including amplitude of eustatic sea-level variation versus time, and two shoreline positions of the latter chart are found differently. One is determined before compaction and is the true shoreline position and the other is determined after compaction and is the position identified by Vail et al. (1977). Fig. 18 shows the horizontal location of the point of greatest onlap, break-in-slope of shelf and furthest extent of sediment deposition.

(2) *Number of horizontal points*. The distance between each point, the horizontal resolution, is determined by the width of shelf and shelf-derived sediment in the basin and matches the length of the model, as defined by the start and end locations, divided by the number of horizontal positions desired.

(3) *Height and length of sediment triangles*. The quantity of sand and shale deposited within a particular time interval and their vertical and lateral distribution can be determined in the following way.

(a) Using at least two wells along the line of the simulation, in conjunction with a seismic cross-section, determine the amount of sediment in terms of the cross-sectional area of the sediment body (Fig. 10).

(b) Next calculate the percentage of sand and the percentage of shale within this sediment volume. Using these percentages and the total volume of the sediment, one can determine the volume and/or area of sand (A_s) deposited and the volume and/or area of shale (A_c) deposited per time step. For instance the volumes of sand and shale are divided by the number of time steps. The sand and shale should be uncompacted following this last calculation. This is calculated in the following way:

$$d_1 = d_2(1-\phi_2)/(1-\phi_1)$$

where d_1 = uncompacted thickness, d_2 = compacted thickness, ϕ_2 = compacted porosity, ϕ_1 = uncompacted porosity.

(c) Next the length of the triangle representing the volume of sand and shale deposited within the time interval of the simulation is derived. The shale triangle length (L_c) is a fraction of the length of the total sediment body being simulated. The exact fraction depends upon the configuration of the depositional surface and the amplitude of sea-level variations, and is determined by iterating from an initial estimate. A reasonable initial estimate of the shale length would be half

the length of the entire sediment body with the height $h_s = 2A_c/L_c$.

The sand triangle length (L_s) would be less than half the shale triangle, with height $h_s = 2A_s/L_s$.

(4) *Subsidence and the location of the hinge point about which thermal subsidence takes place.* The hinge point is a position at which no thermal subsidence takes place. Seaward of the hinge point subsidence increases linearly. This subsidence is assumed due to thermal cooling causing the crust to contract and so subside. The position of the hinge point is determined from a seismic section at the location where sediments cease to thin rapidly landward. The subsidence rate, however, is determined from an analysis of the geohistory curves (Fig. 7).

(5) *Bypass angle.* The angle beyond which sediment is not deposited we fixed at 2°, but this may be changed to suit the operator. We chose 2° since modern continental slopes seldom exceed this.

(6) *Erosion.* At sea-level lows the shelf is exposed above sea level. The maximum area or volume of sediment eroded for each time interval while sea level is low and below the shelf is set at zero unless changed by the operator. Evidence from modern coastal plains suggests that unless the coastal plain is uplifted and acquires angles in excess of 5°, erosion to all intents and purposes tends to be non-existent, and deposition may even occur.

(7) *The geometry of the initial surface.* This is identified by using vertical and horizontal coordinates, and these are determined from seismic data from which a time-to-depth conversion is made, or from a combination of seismic data and wells. Clearly the present configuration will not serve except as a first guess. We suggest iterative trial and error.

(8) *Eustasy.* It was our hope that eustatic sea-level variations could be derived from the integration of data from many wells from all over the world (Guidish et al., 1984). However, as discussed in the body of the paper, we are unable to separate changes in eustasy from sediment accumulation effects though relative magnitudes can be guessed at if traced from basin to basin. Initially curves of Vail et al. (1977) and Vail and Hardenbol (1979), or Pitman's (1978) curves, or, alternatively, curves based on the operator's initial geologic interpretation of seismic data, can be used to estimate sea-level changes. A different sea-level curve can then be found by varying the initial guess (along with the other program inputs) in the simulation geometry. A discussion of the derivation of sea level from burial history via the way outlined by Vail et al. (1977) is given in Guidish et al. (1984).

APPENDIX II

The purpose of this portion of the paper is to spell out the detailed mathematics of how laterally varying onlap sequences are related to sediment fill, sea-level rise and fall, tectonic subsidence and water level variations in a basin.

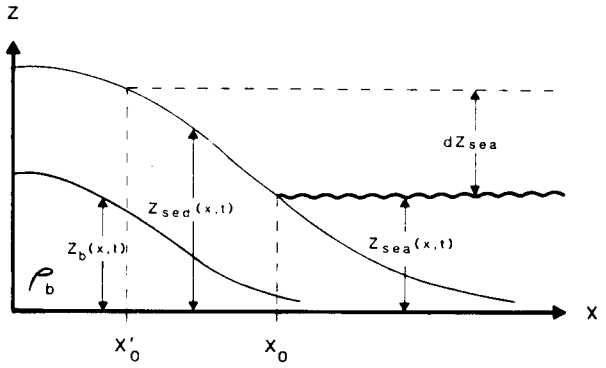

Fig. 19. Diagram for foreward model of sediment accumulation in response to sedimentation rates, tectonic movement and eustatic sea level changes.

We start at some instant of time t with a basin filled as shown (Fig. 19).

In the time interval t to $t+\mathrm{d}t$, add the solid grammage:

$$\mathrm{d}m_s = \rho_1(x)[1-\varphi_1(x)]\,\mathrm{d}z_{sed}$$

and the water grammage:

$$\mathrm{d}m_w = \rho_w\varphi_1(x)\,\mathrm{d}z_{sed}$$

and the sea level grammage:

$$\mathrm{d}m_{sea} = \rho_w z_{sea}$$

with $\mathrm{d}z_{sed} = 0$ to the left of X_0. Here $\rho_L(x)$ is the lithology-dependent grain density, $\phi_L(x)$ the surface porosity, $\mathrm{d}z_{sed}$ the increase in thickness of sediment at position x, $\mathrm{d}z_{sea}$ the increase in water depth (sea level) which is independent of x (for the moment) to the right of the onlap point x_0, and shoals to the left as sketched.

Since all our calculations are isostatically compensated, in order to establish the levels of sea level, sediment thickness etc. at the next time stage of deposition, we break the calculation into three steps: (1) the compaction of the sediments underlying the added material, holding the basement fixed in position; (2) the vertical compensation movement of the basin; (3) the motion of the point of greatest onlap as a consequence of (1) and (2); (4) proceed to the differential limit as $\mathrm{d}t \to 0$, appropriate for continuous deposition.

Compaction

As a consequence of increased solid grammage deposited, the underlying sediments are compacted such that an element of sediment of lithology l which was at coordinates (z, x) at time t, moves to coordinates $(z - \Delta z, x)$ at time $t+\mathrm{d}t$ and an element of lithology l at $(z + H, x)$ moves to $(z + H - \Delta H, x)$ at $t+\mathrm{d}t$.

Skeletal matter being conserved we have:

$$\int_z^{z+H}[1-\varphi_1(z',x)]\,dz'$$
$$=\int_{z-\Delta z}^{z-\Delta z+H-\Delta H}[1-\varphi_1(z',x)]\,dz'$$

with $\Delta z = 0$ for an element sited on $z = z_b$ at time t.

For a given law of porosity with depth (we use an exponential variation of porosity with depth throughout but the calculations can be redone for any specified porosity with depth variation) we write:

$$\varphi_1(z, x) = \varphi_1(x)\exp[-(z_{sed}-z)/a_1]$$

so that:

$$dH_1 = dz\varphi_{1b}\exp[-(z_b-z)/a_1](e^{H_1/a_1}-1)$$
$$\times\{1-\varphi_{1b}\exp[-(z_b-z-H_1)/a_1]\}^{-1}$$

where:

$$\varphi_{1b} = \varphi_1(x)\exp[-(z_s-z_b)/a_1]$$

The base of the L^{th} layer is at $z_L = z_{L-1} + H_{L-1}$ at time t, and at $z_L - dz_L = z_{L-1} - dz_{L-1} + d\ H_{L-1}$ at time $t+dt$.

The total *increase* in sediment thickness at $t+dt$ at position x is:

$$dh = dz_{sed} - \sum_{l=1}^{N} dH_l$$

where N is the number of sedimentary layers deposited prior to time t. The height of the sediments *above* the basement at z_b at time $t+dt$ is:

$$h = dh + \sum_{l=1}^{N} H_l$$

The grammage of water *lost* from the Lth layer in time t to $t+dt$ is:

$$\Delta m_l = \rho_w\, dH_l$$

so that the total lost grammage of water is:

$$\Delta m_w = \rho_w \sum_{l=1}^{N} dH_l$$

The net balance of pore water in t to $t+dt$ is then

$$\delta m_w = \rho_w\varphi_L(x)\,dz_{sed} - \Delta m_w$$

In an infinite ocean this pore water change provides no shift in sea level. It corresponds to a shift in weight on the underlying mantle. The increase in mass in t to $t+dt$ at x acting on the mantle is:

$$dw = dm_s + \delta m_w + \rho_w\, dz_{sea}$$

while the sediment column height above basement increases by dh.

Basement motion

As a consequence of the increase in weight, the isostatic basement position $z_b\ (x, t)$ will move. At x let the basement move in time t to $t+dt$ from z_b to $z_b - dz_b$. Then at the end of $t+dt$ the column sedimentary height is $h+dh$ above basement, while the water height above sediment is:

$$dz_{sea} + dz_b = d\mu$$

Thus measured from the basinal coordinates sketched in Fig. 19 we have PE_b (= potential energy of basement material) given by

$$PE_b = g\rho_m\int_0^{z_b-dz_b} z'\,dz',$$

$$PE_{sed} = g\int_{z_b-dz_b}^{z_b-dz_b+h+dh} z'$$
$$\times\{\rho_L(z')[1-\varphi_L(z')]+\rho_w\varphi_L(z')\}\,dz'$$

$$PE_{water} = g\rho_w\int_{z_b-dz_b+h+dh}^{z_b-dz_b+h+dh+d\mu} z'\,dz'$$

The total potential energy, PE, is then

$$PE = PE_b + PE_{sed} + PE_{water}$$

Isostatic equilibrium is reached when the change of PE w.r.t. dz_b is minimum, i.e., when $\partial PE/\partial\, dz_b = 0$

This occurs at $t+dt$ when:

$$\rho_b(z_b-dz_b)+\{\rho_L(x,t+dt)[1-\varphi_L(x,t+dt)]$$
$$+\rho_w\varphi_L(x,t+dt)\}(z_b-dz_b+h+dh)$$
$$-\{\rho_L(z=z_b-dz_b,x)[1-\varphi_L(z=z_b-dz_b,x)]$$
$$+\rho_w\varphi_L(z_b-dz_b,x)\}(z_b-dz_b)+\rho_w\,d\mu=0$$

Now prior to increasing the load, at time t we have:

$$\rho_b z_b+\{\rho_L(x,t)[1-\varphi_L(x,t)]$$
$$+\rho_w\varphi_L(x,t)\}(z_b+h)$$
$$-z_b\{\rho_L(z=z_b,x)[1-\varphi_L(z=z_b,x)]$$
$$+\rho_w\varphi_L(z=z_b,x)\}=0$$

Since the basement porosity changes as a result of added load but the basement lithology does not we have:

$$\rho_L(z=z_b,x)=\rho_L(z=z_b-dz_b,x)$$

Then, by subtraction, we obtain:

$$-\rho_b\,dz_b+\rho_w(dz_b+dz_{sea})+dh\rho_{sed}(x,t+dt)$$
$$-dz_b\rho_{sed}(x,t+dt)$$
$$+(z_b+h)[\rho_{sed}(x,t+dt)-\rho_{sed}(x,t)]$$
$$+dz_b\rho_{sed}(z=z_b,x)$$
$$-[\rho_L(z=z_b,x)-\rho_w]\frac{\partial\varphi_L(z_b,x)}{\partial z_b}dz_b=0$$

i.e.:

$$dz_b\left\{\rho_b-\rho_w+\rho_{sed}(x,t+dt)-\rho_L(z=z_b,x,t)+z_b\frac{\partial\varphi_L(z_b,x)}{\partial z_b}[\rho_L(z=z_b,x)-\rho_w]\right\}$$
$$=\rho_w\,dz_{sea}+dh\rho_{sed}(x,t+dt)+(z_b+h)\times[\rho_{sed}(x,t+dt)-\rho_{sed}(x,t)]$$

Hence we determine the basement motion dz_b in the time interval t to $t+dt$ due to sediment and water load. If, in addition, there are tectonic forces at play causing a downshift in basement position dz_{tect}, then the total basement response in t to $t+dt$ is:

$$dz_{total}=dz_b+dz_{tect}$$

$$z_b(t)=\int_0^t\frac{dz_{total}}{dt}dt$$

so that:

$$z_b(t+dt)=z_b(t)-dz_{total}$$

Sediment thickness and onlap

At the end of time interval t to $t+dt$ the basement at x is now at position z_b $(t+dt)$, the sedimentary column is of height $h'=h+dh$ and the water depth above the sediment is increased by $dz_{sea}+dz_{total}$.

At time t the height of the sea level above the basement (at z_b) is H_{sea} (old) $=z_{sea}-z_b$. At time $t+dt$ the height of the sea level above the new basement (at z_b-dz_{total}) is:

$$H_{sea}(t+dt)=z_{sea}+dz_{sea}-(z_b-dz_{total})$$
$$=H_{sea}(t)+dz_{sea}+dz_{total}$$

Height of the sea level above the new sediment column (of thickness $h+dh$) is

$$H(t+dt)=H_{sea}+dz_{sea}+dz_{total}-(h+dh)$$

The base of a sedimentary layer, layer L, at z, x at time t is now at

$$z'=z-dz-z_b(t+dt)$$

above the new basement position.

At time t the point of greatest onlap, x_p, was where $H_{sea}(t)=H(t)$, i.e. $z_{sea}-z_b=H(t)$.

At time $t+dt$ the point of greatest onlap has moved to x_p+dx_p where the sea-level height above basement equals the sediment column height above basement, i.e. such that:

$$H(t+dt,x_p+dx_p)=0$$

Now:

$$H(t+dt,x)=H_{sea}(t,x)+dz_{sea}(x,t)+dz_{total}(t,x)-h(t,x)-dh$$

and:

$$h(t,x_p+dx_p)=h(t,x_p)+dx_p\frac{\partial h(t,x_p)}{\partial x_p}$$

while:

$$H_{sea}(t,x_p+dx_p)=0$$

so that shift in point of greatest onlap in t to $t+dt$ is:

$$dx_p=\left\{[dh-dz_{sea}-dz_{total}]/\left[\frac{\partial h(t,x_p)}{\partial x_p}\right]\right\}_{x=x_p+dx_p}$$

Note that motion of the point of greatest onlap is determined not only by sediment increase, sea-level shift and basinal drop under sediment load plus tectonics but also by the *slope* of the compacted sedimentary layer surface at the point of greatest onlap, $\partial h(t,x_p)/\partial x_p$.

REFERENCES

Agassiz, L., 1840. Etudes sur les glaciers. Neuchâtel, (privately published).

Aharon, P., 1984. 140,000-yr isotope climatic record from raised coral reefs in New Guinea. Nature, 304: 720–723.

Airy, G.B., 1885. On the computation of the effect of the attraction of the mountain-masses as disturbing the apparent astronomical latitude of stations at geodetic surveys. Phil. Trans. R. Soc. Lond., 145: 101–104.

Aen, J.R.L., 1964. Studies in fluviatile sedimentation: six cyclothems from the Lower Old Red Sandstone, Anglo-Welsh Basin. Sedimentology, 3: 163–198.

Bachmann, G.H. and Koch, K., 1983. Alpine Front and Molasses Basin, Bavaria. In: A.W. Bally (Editor), Seismic Expression of Structural Styles. Am. Assoc. Pet. Geol., Studies in Geology Series, No. 15, Vol. 3, pp. 3.4-1-27.

Bally, A.W., 1981. Basins and subsidence. Am. Geophys. Union Geodyn. Ser., 1: 5–20.

Barrell, J., 1917. Rhythms and the measurements of geologic time. Bull. Geol. Soc. Am., 28: 745–904.

Beaumont, C., 1981. Foreland basins. Geophys. J. R. Astron. Soc., 65: 291–329.

Berger, A.L., 1976. Obliquity and precession for the last 5,000,000 years. Astron. Astrophys., 5: 127–135.

Berger, A.L., 1978. Long-term variations of caloric insolation resulting from the Earth's orbital elements. Quaternary Res., 9: 139–167.

Beukes, N.J., 1977. Transition from siliciclastic to carbonate sedimentation near base of the Transvaal Super group, Northern Cape Province, South Africa. Sediment. Geol., 18: 201–221.

Bloom, A.L., Broecker, W.S., Chappell, J.M.A., Matthews, R.K. and Mesolella, K.J., 1974. Quaternary

sea level fluctuations on a tectonic coast: new $^{230}Th/^{234}U$ dates from the Huon Peninsula, New Guinea. Quaternary Res., 4: 185–205.

Bomford, G., 1971. Geodesy. Oxford Press, London, 2nd ed., pp. 441–443.

Bond, G., 1976. Evidence for continental subsidence in North America during the Late Cretaceous global submergence. Geology, 4: 557–560.

Bond, G., 1978a. Evidence for Late Tertiary uplift of Africa relative to North America, South America, Australia and Europe. J. Geol., 86: 47–65.

Bond, G., 1978b. Speculations on real seal sea-level changes and vertical motions of continents at selected times in the Cretaceous and Tertiary Periods. Geology, 6: 247–250.

Broecker, W.S., 1966. Absolute dating and the astronomical theory of glaciation. Science, 151: 299–304.

Broecker, W.S. and Van Donk, J., 1970. Insolation changes, ice volumes, and the O^{18} in deep-sea cores. Rev. Geophys. Space Phys., 8: 169–198.

Buffler, R.T., Shipley, T.H. and Watkins, J.S., 1978. Blake continental margin. Am. Assoc. Pet. Geol. Seismic Line, 2.

Busch, R.M., 1983. Sea level correlation of punctuated aggradational cycles (PAC's) of the Manlius Formation, Central New York. Northeast. Geol., 5: 82–91.

Chambers, R., 1848. Ancient sea-margins, as memorials of changes in the relative level of land and sea (quoted by Suess, 1906).

Chappell, J., 1974. Geology of coral terraces, Huon Peninsula, New Guinea: a study of Quaternary tectonic movements and sea level changes. Geol. Soc. Am. Bull., 85: 553–570.

Chappell, J. and Shackleton, N.J., 1986. Oxygen isotopes and sea level. Nature, 324: 137–140.

Chappell, J. and Veeh, H.H., 1978. Late Quaternary tectonic movements and sea level changes at Timor and at Atauro Island. Geol. Soc. Am. Bull., 89: 356–368.

Cogley, J.G., 1981. Late Phanerozoic extent of dry land. Nature, 291: 56–58.

Cogley, J.G., 1984. Continental margins and extent and number of the continents. Rev. Geophys. Space Phys., 22: 101–122.

Cook, F.A., Brown, L.D., Kaufman, S. and Oliver, J.E., 1983. The COCORP seismic reflection traverse across the Southern Appalachians. Am. Assoc. Pet. Geol. Stud., 14, 61 pp.

Crain, W.E., Mero, W.E. and Patterson, D., 1985. Geology of the Point Arguello discovery. Am. Assoc. Pet. Geol. Bull., 69: 537–545.

Curnelle, R. and Marco, R., 1983. Reflection profiles across the Aquitaine Basin (North Pyrenean Basin). In: A.W. Bally (Editor), Seismic Expression of Structural Styles. Am. Assoc. Pet. Geol., Studies in Geology Series, No. 15, Vol 1, pp. 1.2-3-1.

De Pratter, C.B. and Howard, J.D., 1981. Evidence for a sea-level lowstand between 4500 and 2400 BP on the southeast coast of the United States. J. Sediment. Petrol., 51: 1287–1295.

Dimian, M.V., Gray, R., Stout, J. and Wood, B., 1983. Hudson Bay Basin. In: A.W. Bally (Editor), Seismic Expression of Structural Styles. Am. Assoc. Pet. Geol. Studies in Geology Series, No. 15, Vol. 2, pp. 2.2-4-1.

Erxleben, A.W. and Carnahan, G., 1983. Slick Ranch area, Starr County, Texas. In: A.W. Bally (Editor), Seismic Expression of Structural styles. Am. Assoc. Pet. Geol., Studies in Geology Series, No. 15, Vol. 2, pp. 2.3-1-22.

Eyged, L., 1956. Determination of changes in the dimensions of the Earth from paleogeographic data. Nature, 173: 534.

Fairbanks, R.G. and Matthews, R.K., 1978. The marine oxygen isotope record in Pleistocene coral, Barbados, West Indies. Quaternary Res., 10: 181–196.

Falvey, D.A., 1974. The development of continental margins in plate tectonic theory. Aust. Pet. Expl. Assoc. J., 14: 95–106.

Ferm, J.C., 1970. Allegheny deltaic deposits. In: J.P. Morgan (Editor), Deltaic Sedimentation Modern and Ancient. SEPM Spec. Publ., 15: 246–255.

Fillon, R.H., 1984. Continental glacial stratigraphy, marine evidence of glaciation and insights into continental–marine correlations. In: Nancy Healy-Williams (Editor), Principles of Pleistocene Stratigraphy applied to the Gulf of Mexico. IHRDC, Boston, pp. 149–206.

Fillon, R.H. and Williams, D.F., 1983 . Glacial evolution of the Plio-Pleistocene: role of continental and arctic ice sheets. Palaeogeogr., Palaeoclimatol., Palaeoecol., 43: 7–33.

Fillon, R.H. and Williams, D.F., 1984. Dynamics of meltwater discharge from Northern Hemisphere ice sheets during the last deglaciation. Nature, 310: 674–677.

Fischer, A.G., 1964. The Lofer cyclothem of the Alpine Triassic, Kansas Geol. Surv. Bull., 169: 107–149.

Forney, G.G., 1975. Permo-Triassic sea level change. J. Geol., 83: 773–779.

Fox, F.G., 1983. Structure sections across the Parry Islands fold belt and the Vescy Hamilton Salt Wall, Arctic Archipelago, Canada. In: A.W. Bally (Editor), Seismic Expression of Structural Styles. Am. Assoc. Pet. Geol., Studies in Geology Series, No. 15, Vol. 3, pp. 3.4-1-54.

Gairud, H. et al., 1978. The Jan Mayen Ridge, Synthesis of geological knowledge and new data. Oceanol. Acta, 1: 335–358.

Gamboa, L.A., Truchan, M. and Stoffa, P.L., 1985. Middle and Upper Jurassic depositional environments at outer shelf and slope of Baltimore Canyon Trough. Am. Assoc. Pet. Geol. Bull., 69: 610–621.

Gardner, G.H.F., Gardner, L.W. and Gregory, A.R., 1974. Formation velocity and density; the diagnostic basis for stratigraphic traps. Geophysics, 39: 770–780.

Goodwin, P.W. and Anderson, E.J., 1985. Punctuated aggradational cycles: a general hypothesis of episodic stratigraphic accumulation. J. Geol., 93: 515–534.

Grabau, A.W., 1936. Paleozoic Formations in the Light of the Pulsation Theory, 1. Heath and Co., New York, N.Y., 83 pp.

Guidish, T.M., Lerche, I., Kendall, C.G.St.C. and O'Brien, J.J., 1984. Relationship between Eustatic Sea level changes and basement subsidence. Am. Assoc. Pet. Geol., 68: 164–177.

Gutenberg, B., 1941. Changes in sea level, post glacial uplift, and mobility of the earth's interior. Bull. Geol. Soc. Am., 52: 721–772.

Hallam, A., 1963. Major epeirogenic and eustatic changes since the Cretaceous, and their possible relationship to crustal structure. Am. J. Sci., 261: 397–423.

Hallam, A., 1969. Tectonism and eustasy in the Jurassic. Earth. Sci. Rev., 5: 45–68.

Hallam, A., 1977. Secular changes in marine inundation of USSR and North America through the Phanerozoic. Nature, 269: 769–772.

Hallam, A., 1981. A revised sea-level curve from the Early Jurassic. J. Geol. Soc. Lond., 138: 735–743.

Hallam, A., 1984. Pre-Quaternary sea-level changes. Ann. Rev. Earth Planet. Sci., 12: 205–243.

Hamberg, L.R., 1983. Seismic profiles and a stratigraphic trap East Texas field. In: A.W. Bally (Editor), Seismic Expression of Structural Styles. Am. Assoc. Pet. Geol., Studies in Geology Series, No. 15, Vol. 1, pp. 1.2-2-15.

Hancock, J.M. and Kauffman, E.G., 1979. The great transgressions of the Late Cretaceous. J. Geol. Soc. Lond., 136: 175–186.

Hardenbol, J., Vail, P.R. and Ferrer, J., 1981. Interpreting paleoenvironments, subsidence history, and sea level changes of passive margins from seismic and biostratigraphy. Oceanol. Acta, Proc. 26th Int. Geol. Congr. Geology of Continental Margins, Symp., Paris, 7-17, 1980, pp. 33–44.

Harding, T.P., 1985. Seismic characteristics and identification of negative flower structures, positive flower structures and positive structural inversion. Am. Assoc. Pet. Geol. Bull., 69: 582–600.

Harding, T.P. and Lowell, J.D., 1983. Structural styles, their plate tectonic habitats and hydrocarbon traps in petroleum provinces. In: A.W. Bally (Editor), Seismic Expression of Structural Styles. Am. Assoc. Pet. Geol., Studies in Geology Series, No. 15, Vol. 1, pp. 1–24.

Harding, T.P., Gregory, R.F. and Stephens, L.H., 1983. Convergent Wrench Fault and positive flower structure, Ardmore Basin, Oklahoma. In: A.W. Bally (Editor), Seismic Expression of Structural Styles. Am. Assoc. Pet. Geol., Studies in Geology Series, No. 15, Vol. 3, pp. 4.2-13.

Harland, W.B., Cox, A.V., Llewellyn, P.G., Pickton, C.A.G., Smith, A.G. and Walters, R., 1982. A Geologic Time Scale. Cambridge University Press, 128 pp.

Harms, J.C., 1974. Brushy Canyon Formation, Texas: A deep-water density current deposit. Geol. Soc. Am. Bull., 85: 1763–1784.

Harris, P.M., Frost, S.H., Seiglie, G.A. and Schneidermann, N., 1984. Regional unconformities and depositional cycles, Cretaceous of Arabian Peninsula. In: J.S. Schlee (Editor), Inter-regional Unconformities and Hydrocarbon Accumulations. Am. Assoc. Pet. Geol. Mem., 36: 67–80.

Harrison, C.G.A., Brass, G.W., Saltzman, E., Sloan, J. II., Southam, J. and Whitman, J.M., 1981. Sea level variations, global sedimentation rates and the hypsographic curve. Earth Planet. Sci. Lett., 54: 1–16.

Helland-Hansen, W., Kendall, C.G.St.C., Nakayama, K. and Lerche, I., 1986. Simulation of basin margin sedimentation in response to crustal movement, eustasy, and sediment accumulation rates. In prep.

Hellinger, S.J. and Sclater, J.G., 1983. Some comments on two layer extentional models for the evolution of sedimentary basins. J. Geophys. Res., 88: 8251–8269.

Horne, J.C. and Ferm, J.C., 1976. Carboniferous Depositional environments: Eastern Kentucky and Southern West Virginia, a Field Guide. Dept. Geol., University of South Carolina, 129 pp.

James, N.P., 1979. Shallowing-upward sequences in carbonates. In: R.G. Walker (Editor), Facies Models. Geoscience Canada Reprint Series, 1: 109–119.

Kauffman, E.G., 1977. Geological and biological overview: Western Interior Cretaceous Basin. Mt. Geol., 14: 75–99.

King, P.B., 1948. Geology of Southern Guadalupe Mountains, Texas. U.S. Geol. Surv. Prof. Pap., 215: 183 pp.

Kirschner, C.E., Gryc, G. and Molenaar, C.M., 1983. Regional seismic lines in the National Petroleum Reserve in Alaska. In: A.W. Bally (Editor), Seismic Expression of Structural Styles. Am. Assoc. Pet. Geol., Studies in Geology Series, No. 15, Vol. 1, pp. 1.2.5-1.

Klein, G.DeV., 1970. Tidal origin of a Precambrian quartzite—The Lower Fine-grained Quartzite (Middle Dalradian) of Islay, Scotland. J. Sediment. Petrol., 40: 973–985.

Kominz, M.A., 1984. Oceanic Ridge volumes and sea level change—an error analysis. In: J.S. Schlee (Editor), Interregional Unconformities and Hydrocarbon Accumulation. Am. Assoc. Pet. Geol. Mem., 36: 108–128.

Kossinna, E., 1921. Die Tiefen des Weltmeeres. Berlin

Univ., Inst. Meereskunde, Veröff. Geogr. Naturwiss, N.S., No. 9, 70 pp.

Kossinna, E., 1933. Die Erdoberflache. In B. Gutenberg (Editor), Handbuch der Geophysik, 2. Aufbau der Erde. Gebrüder Borntraeger, Berlin, Absch. VI, pp. 809–954.

Kuenen, Ph.H., 1939. Quantitative estimations relating to eustatic movements. Geol. Mijnbouw, 8: 194–201.

Matthews, R.K., 1984a. Dynamic Stratigraphy, an Introduction to Sedimentation and Stratigraphy. Prentice-Hall, Englewood Cliffs, N.J., 489 pp.

Matthews, R.K., 1984b. Oxygen-isotope record ocean—volume history: 100 million years of glacio-eustatic sea level fluctuation. In: J.S. Schlee (Editor), Interregional Unconformities and Hydrocarbon Accumulation. Am. Assoc. Pet. Geol. Mem., 36: 97–107.

McKenzie, D., 1978. Some remarks on the development of sedimentary basins. Earth Planet. Sci. Lett., 40: 25–32.

McKerrow, W.S., 1979. Ordovician and Silurian changes in sea level. J. Geol. Soc. Lond., 136: 137–145.

Mesolella, K.J., Matthews, R.K., Broecker, W.S. and Thurber, D.L., 1969. The astronomical theory of climatic change: Barbados data. J. Geol., 77: 250–274.

Miall, A.D., 1986. Eustatic sea-level changes interpreted from seismic stratigraphy: a critique of the methodology with particular references to the North Sea record. Am. Assoc. Pet. Geol. Bull., 70: 131–137.

Middleton, M.F., 1984. Seismic geohistory analysis—a case history from the Canning Basin, Western Australia. Geophysics, 49: 333–343.

Milankovich, M., 1941. Canon of insolation and the Ice-Age problems. R. Serbian Acad. Spec. Publ., 132, Sect. of Mathematical and Natural Sciences, 33 (translated U.S. Dept. of Commerce).

Moore, W.S., 1982. Late Pleistocene sea level history: In: M. Ivanovich and R. Harmon (Editors), Uranium-Series Disequilibrium: Applications to Environmental Problems in the Earth Sciences. Oxford University Press, pp. 481–496.

Morrison, L., 1985. The day time stands still. New Sci., 1462: 20–21.

Mörner, N.A., 1983. Sea levels: In: R. Gardner and H. Scoging (Editors), Megageomorphology. Clarendon Press, Oxford, pp. 73–91.

Norton, M.A., 1983. Kemmerer Area, Lincoln County Wyoming, 1983. In: A.W. Bally (Editor), Seismic Expression of Structural Styles. Am. Assoc. Pet. Geol., Studies in Geology Series, No. 15, Vol. 3, pp. 3.4-1-45.

Nunn, J.A., Sleep, N.H. and Moore, W.E., 1984. Thermal subsidence and generation of hydrocarbons in Michigan basin. Am. Assoc. Pet. Geol. Bull., 68: 296–315.

Palmer, A.R., 1983. The decade of North American geology, 1983, geologic time scale. Geology, 11: 501–564.

Parkinson, N. and Summerhayes, C., 1985. Synchronous global sequence boundaries. Am. Assoc. Pet. Geol. Bull., 69: 658–687.

Parsons, B. and Sclater, J.G., 1977. An analysis of the variations of ocean floor bathymetry and heat flow with age. J. Geophys. Res., 82: 803–827.

Phelps, E.H. and Roripaugh, C.C., Jr., 1983. Carbonate shelf, Central Louisiana. In: A.W. Bally (Editor), Seismic Expression of Structural Styles. Am. Assoc. Pet. Geol., Studies in Geology Series, No. 15, Vol. 1, pp. 1.2.4-1.

Pieri, M., 1983. Three seismic profiles through the Po Plain. In: A.W. Bally (Editor), Seismic Expression of Structural Styles. Am. Assoc. Pet. Geol., Studies in Geology Series, No. 15, Vol. 3, pp. 3.4-1-27.

Pitman, W.C., 1978. Relationship between sea-level change and stratigraphic sequences of passive margins. Geol. Soc. Am. Bull., 89: 1389–1403.

Poag, C.W. and Schlee, J.S., 1984. Depositional sequences and stratigraphic gaps on submerged Atlantic margin. In: J.S. Schlee (Editor), Interregional Unconformities and Hydrocarbon Accumulation. Am. Assoc. Pet. Geol. Mem., 36: 65–182.

Rafavich, F., Kendall, C.G.St.C. and Todd, T.P., 1984. The relationship between acoustic properties and the petrographic character of carbonate rocks. Geophysics, 49: 1622–1636.

Ricci-Lucchi, F., 1975. Depositional cycles in two turbidite formations of northern Apennines (Italy). J. Sediment. Petrol., 45: 3–42.

Rona, P.A., 1973. Relations between rates of sediment accumulation on continental shelves, sea floor spreading, and eustacy inferred from central North Atlantic. Geol. Soc. Am. Bull., 84: 2851–2872.

Royden, L., Sclater, J.G. and Von Herzen, R.P., 1980. Continental margin subsidence and heat flow; important parameters in formation of petroleum hydrocarbons. Am. Assoc. Pet. Geol. Bull., 64: 173–187.

Ruddiman, W.F. and McIntyre, A., 1981. Oceanic mechanism for amplification of the 23,000-year ice-volume cycle. Science, 212: 617–627.

Schlee, J.S and Fritsch, J., 1983. Seismic stratigraphy of the Georges Bank Basin complex, offshore New England. In: J.S. Watkins and C.L. Drake (Editors), Studies in Continental Marine Geology. Am. Assoc. Pet. Geol. Mem., 34: 223–251.

Schuchert, C., 1916. Correlation and chronology in geology in the basis of paleogeography. Bull. Geol. Soc. Am., 27: 491–514.

Seiglie, G.A. and Baker, M.B., 1984. Relative sea-level changes during the Middle and Late Cretaceous from Zaire to Cameroon (Central West Africa). In: J.S. Schlee (Editor), Interregional Unconformities and Hydrocarbon Accumulation. Am. Assoc. Pet. Geol. Mem., 36: 81–88.

Seiglie, G.A. and Moussa, M.T., 1984, Late Oligocene-Pliocene transgression—regression cycles of sedimentation in Northwestern Pureto Rico: In: J.S. Schlee (Editor), Interregional Unconformities and Hydrocarbon Accumulation. Am. Assoc. Pet. Geol. Mem., 36: 89–96.

Sengbush, R.L., Lawrence, P.L. and McDonal, F.J., 1961. Interpretation of synthetic seismograms. Geophysics, 26: 138–157.

Shackleton, N.J. and Opdyke, N.D., 1973. Oxygen isotope and paleomagnetic stratigraphy of Equatorial pacific core V28-238: oxygen isotope temperature and ice volumes on a 10^5 year and 10^6 year scale. Quaternary Res., 3: 39–55.

Sloss, L.L., 1963. Sequences in the cratonic interior of North America. Geol. Soc. Am. Bull., 74: 93–113.

Sloss, L.L., 1972. Synchrony of Phanerozoic sedimentary-tectonic events of the North American craton and the Russian Platform. 24th Int. Geol. Congr. Sect. 6, pp. 24–32.

Sloss, L.L., 1984. Comparative anatomy of cratonic unconformities. In: J.S. Schlee (Editor), Interregional Unconformities and Hydrocarbon Accumulation. Am. Assoc. Pet. Geol. Mem., 36: 7–36.

Sloss, L.L. and Speed, R.C., 1974. Relationships of cratonic and continental margin tectonics episodes. In: W.R. Dickinson (Editor), Tectonics and Sedimentation. Soc. Econ. Paleontol. Miner. Spec. Publ., 22: 98–119.

Southam, J. and Whitman, J.M., 1981. Sea level variations, global sedimentation rates and the hypsographic curve. Earth Planet. Sci. Lett., 54: 1–16.

Steckler, M.A. and Watts, A.B., 1978. Subsidence of the Atlantic-type continental margin off New York. Earth Planet. Sci. Lett., 41: 1–13.

Steinen, R.P., Harris, R.S. and Matthews, R.H., 1973. Eustatic low stand of sea level between 125,000 and 105,000 B.P. Evidence from the subsurface of Barbados, West Indies. Geol. Soc. Am. Bull., 84: 63–70.

Stille, H., 1924. Grundfragen der vergleichenden Tektonik. Borntraeger, Berlin, 443 pp.

Stone, D.S., 1983a. North Fork Area, Powder River Basin, Wyoming. In: A.W. Bally (Editor), Seismic Expression of Structural Styles. Am. Assoc. Pet. Geol., Studies in Geology Series, No. 15, Vol. 3, pp. 3.2-2-15.

Stone, D.S., 1983b. Seismic Profile: South Elk Basin. In: A.W. Bally (Editor), Seismic Expression of Structural Styles. Am. Assoc. Pet. Geol., Studies in Geology Series, No. 15, Vol. 3, pp. 3.2.2-20.

Suess, E., 1906. The Face of the Earth, 2. Clarendon Press, Oxford, 556 pp.

Suzuki, J., 1983. The volcanic mound. In: A.W. Bally (Editor), Seismic Expression of Structural Styles. Am. Assoc. Pet. Geol., Studies in Geology Series, No. 15, Vol. 1, pp. 1.3-15.

Thomson, A., 1983. Salt rollers—East Texas Salt Basin. In: A.W. Bally (Editor), Seismic Expression of Structural Styles. Am. Assoc. Pet. Geol., Studies in Geology Series, No. 15, Vol. 2, pp. 2.3-2-18.

Thorne, J. and Watts, A.B., 1984. Seismic reflectors and unconformities at passive continental margins. Nature, 311 (5984): 365–367.

Umbgrove, J.H.F., 1939. On rhythms in the history of the earth. Geol. Mag., 76: 116–129.

Vail, P.R. and Hardenbol, J., 1979. Sea level changes during Tertiary. Oceans, 22 (3): 71–79.

Vail, P.R. and Todd, R.G., 1981. Northern North Sea Jurassic unconformities, chronostratigraphy and sea level changes from seismic stratigraphy. In: L.V. Illing and G.D. Hobson (Editors), Proceeding of the Petroleum Geology of the Continental Shelf of NW Europe Conf., March 4–6, 1980. London. Heydon and Son Ltd., London, pp. 216–235.

Vail, P.R., Mitchum, R.M., Jr., Todd, R.G., Widmier, J.M., Thompson, S., III., Sangree, J.B., Bubb, J.N. and Hatleilid, W.G., 1977. Seismic stratigraphy and global changes of sea level. In: C.E. Payton (Editor), Seismic Stratigraphy—Applications to Hydrocarbon Exploration. Am. Assoc. Pet. Geol. Mem., 26: 49–212.

Vail, P.R., Hardenbol, J. and Todd, R.G., 1984. Jurassic unconformities, chronostratigraphy and sea level changes from seismic and biostratigraphy. In: J.S. Schlee (Editor), Interregional Unconformities and Hydrocarbon Accumulation, Am. Assoc. Pet. Geol. Mem., 36: 347–363.

Van Hinte, J.E., 1976a. A Jurassic time scale. Am. Assoc. Pet. Geol. Bull., 60: 489–497.

Van Hinte, J.E., 1976b. A Cretaceous time scale. Am. Assoc. Pet. Geol. Bull., 60: 498–516.

Van Hinte, J.E., 1978. Geohistory analysis—application of micropaleontology in exploration geology. Am. Assoc. Pet. Geol. Bull., 62: 201–222.

Van Hinte, J.E., 1983. Synthetic seismic sections from biostratigraphy. In: J.S. Watkins and C.L. Drake (Editors), Studies in Continental Margin Geology. Am. Assoc. Pet. Geol. Mem., 34: 675–685.

Vella, P., 1961. Terms for real and apparent height changes of sea level and parts of the lithosphere. Trans. R. Soc. N. Z., 1: 101–109.

Von Rad, U. and Exon, N.F., 1983. Mesozoic–Cenozoic sedimentary and volcanic evolution of the starved passive margin off Northwest Australia. In: J.S. Watkins and C.L. Drake (Editors), Studies in Continental Margin Geology. Am. Assoc. Pet. Geol. Mem., 34: 253–281.

Walcott, R.I. 1970. Flexural rigidity, thickness, and viscosity of the lithosphere. J. Geophys. Res., 75: 3941–3954.

Walker, R.G. and Harms, J.C., 1971. The "Catskill Delta": a prograding muddy shoreline in central Pennsylvania. J. Geol., 79: 381–399.

Wanless, H.R. and Shepard, F.P., 1936. Sea level and climatic changes related to Late Paleozoic cycles. Bull. Geol. Soc. Am., 47: 1177–1206.

Ward, W.T. and Chappell, J., 1975. Geology of coral terraces, Huon Peninsula, New Guinea: A study of Quaternary tectonic movements and sea level changes: discussion and reply. Geol. Soc. Am. Bull., 86: 1482–1486.

Watkins, J.S. et al., 1976. Southern Gulf of Mexico. Am. Assoc. Pet. Geol., Seismic Line, 1.

Watts, A.B., 1982. Tectonic subsidence, flexure and global changes of sea level. Nature, 297: 469–474.

Watts, A.B. and Steckler, M.S., 1979. Subsidence and eustasy at the continental margin of eastern North America. In: M. Talwani, W. Hay and W.B.F. Ryan (Editors), In Deep Drilling results in the Atlantic Ocean: Continental Margins and Paleoenvironment. Am. Geophys. Union, Ewing Ser., 3: 218–234.

Weimer, R.J., 1984. Relation of unconformities, tectonics and sea-level changes, Cretaceous of Western Interior, USA. In: J.S. Schlee (Editor), Interregional Unconformities and Hydrocarbon Accumulation. Am. Assoc. Pet. Geol. Mem., 36: 7–36.

Wells, A.J., 1960. Cyclic sedimentation: a review. Geol. Mag., 97: 389–403.

Wheeler, H.E., 1958. Time stratigraphy. Am. Assoc. Pet. Geol. Bull., 42: 1047–1063.

Williams, D.F., Moore, W.S. and Fillon, R.H., 1981. Role of glacial Arctic Ocean ice sheets in Pleistocene oxygen isotope and sea level records. Earth Planet. Sci. Lett., 56: 157–166.

Williamson, C.R., 1977. Deep sea channels of the Bell Canyon Formation (Guadalupian), Delaware Basin, Texas-New Mexico. In: M.E. Hileman and S.J. Mazzullo (Editors), Upper Guadalupian Facies, Permian Reef Complex, Guadalupe Mountains, New Mexico and West Texas. Permian Basin Section SEPM, Publ. 77-16, pp. 409–432.

Willumsen, P.S. and Cote, R.P., 1983. Tertiary sedimentation in the southern Beaufort Sea, Canada. In: J.S. Watkins and C.L. Drake (Editors), Studies in Continental Margin Geology, Am. assoc. Pet. Geol. Mem., 34: 283–293.

Wyatt, A.R., 1984. Relationship between continental area and elevation. Nature, 311: 370–372.

[Received June 23, 1986; accepted after revision April 23, 1987]